Bio-Design and Manufacturing (2021) 4:541–567
https://doi.org/10.1007/s42242-020-00119-y

REVIEW

Current researches on design and manufacture of biopolymer-based osteochondral biomimetic scaffolds

Yanen Wang[1,2] · Ying Guo[1,2] · Qinghua Wei[1,2] · Xinpei Li[1,2] · Kang Ji[1,2] · Kun Zhang[1,2]

Received: 24 July 2020 / Accepted: 1 December 2020 / Published online: 1 February 2021

Abstract

Currently, osteochondral (OC) tissue engineering has become a potential treatment strategy in repairing chondral lesions and early osteoarthritis due to the limited self-healing ability of cartilage. However, it is still challenging to ensure the integrity, physiological function and regeneration ability of stratified OC scaffolds in clinical application. Biomimetic OC scaffolds are attractive to overcome the above problems because of their similar biological and mechanical properties with native OC tissue. As a consequence, the researches on biomimetic design to achieve the tissue function of each layer, and additive manufacture (AM) to accomplish composition switch and ultrastructure of personalized OC scaffolds have made a remarkable progress. In this review, the design methods of biomaterial and structure as well as computer-aided design, and performance prediction of biopolymer-based OC scaffolds are presented; then, the characteristics and limitations of AM technologies and the integrated manufacture schemes in OC tissue engineering are summarized; finally, the novel biomaterials and techniques and the inevitable trends of multifunctional bio-manufacturing system are discussed for further optimizing production of tissue engineering OC scaffolds.

Keywords Osteochondral tissue · Biomimetic scaffold · Additive manufacture · Integrated manufacture

Introduction

Cartilage defect is a common cause of disability in individuals over the age of 30, especially for the groups subjected to high-strength exercises and weight-bearing work. Cartilage defects accompanied by severe instability, pain and mobility impairment are usually treated by various clinical therapies from chondrocyte implantation, autograft/allograft implantation, bone marrow simulation to microfracture, etc. [1–4]. However, these therapeutic approaches are generally limited by poor postoperative repair, such as fibro cartilage forming, high morbidity of donor site and inferior durability of prosthetics. The neo cartilage with dysfunction caused by inadequate treatment may even develop into repeated OA, a prevalent degenerative disorder worldwide. It is estimated that 10% of men and 18% of women over 60 years old are to be severely affected by OA [5].

The self-repairing capacity of cartilage is limited by its avascular nature, low metabolic activity, less progenitor cells and growth factors within the dense extracellular matrix (ECM) [6], which further results in the slow integration between cartilage graft and host bed/underlying subchondral bone; during the repair process of tissue, such poor interface significantly affect the stability of host bed surface which ultimately accounts for the failure of transplantation. As a consequence, due to the rich blood supply, nerves and lymphatics in subchondral bone, more attention has been given to OC scaffolds for accelerating interface integrity and cartilage regeneration [7]. The load-bearing OC tissue, possessing a depth-wise transitional structure, is composed of hyaline cartilage (superficial, middle and deep), calcified cartilage and underlying subchondral bone [8]. The gradients of cell phenotype and its associated ECM composition of OC tissue cooperatively modulate cellular fate, which results in naturally varying physiological functionality along distinct tissue regions [9, 10]: hyaline cartilage composed of

Yanen Wang and Ying Guo have contributed equally to this work.

✉ Yanen Wang
wangyanen@nwpu.edu.cn

[1] Department of Mechanical and Electronic Engineering, School of Mechanical Engineering, Northwestern Polytechnical University, Xi'an 710072, China

[2] Institute of Medical Research, Northwestern Polytechnical University, Xi'an 710072, China

water, collagen II, glycosaminoglycans (GAG), buffers the external forces and reduces friction during the motion of skeletal system; subchondral bone with the principal ECM constituents of collagen I and hydroxyapatite (HA) provides mechanical and structural support; calcified cartilage containing HA and collagen II plays a unique role in maintaining the structural continuity [11] and separating cartilage and subchondral bone [12].

The heterogeneous composition and stratified architecture of OC scaffolds are initially realized using traditional manufacturing processes, such as polymeric extraction, particulate leaching, gas foaming, mold casting and phrase separation and freeze-drying, etc. However, OC scaffolds need to be developed to synchronously satisfy the requirements of distinct cell populations [13], and the requirement of temporary mechanical properties and biodegradability to avoid stress shielding phenomenon [14]. Here, it is necessary to ensure the precise contour, mechanical gradient and differing biological properties of OC scaffolds. The accurate imitation of natural OC tissue and processing of suitable bone biomaterials are becoming dramatic challenges encountered by traditional preparation methods of OC reparative scaffolds [15]. In this case, AM technologies have received considerable attention in bone tissue engineering (BTE) because of their professionalism in fabricating the patient-specific bone scaffolds [16] related to chemical components, regeneration ability and mechanical properties [17]. Moreover, computer-aided design has been rapidly developed in order to optimize OC scaffolds with reduced design period and experimental cost. In view of processability, flexibility and cost-effectiveness, polymer-based biomaterials with good biodegradability and biocompatibility [18] have drawn our attention, particularly polymer-based nanocomposites due to the presence of inorganic nHA crystals in bone.

In this review, we summarize research progresses in biomimetic design of polymer-based OC scaffolds, and the application of finite element (FE) method is described as an aided design approach. Then, we concentrate on the manufacturing strategies of OC scaffolds based on AM technologies. Finally, aiming at simplifying the process and solving the existing problems, we analyze the research trend of OC scaffolds in BTE to meet the clinical application standards.

Biomimetic design of OC scaffolds

Physicochemical properties (inner structure, porosity, elastic modulus, hydrophobicity and degradation) of BTE scaffolds are considered crucial in cell behavior and tissue regeneration; specifically, the potential biological functions of scaffolds are mainly reflected by the differentiation of stem cells which depends on the microstructure, mineral contents and mechanical properties of scaffolds [19]. The research focus gradually shifts to biomimetic OC scaffolds which provide favorable microenvironments for tissue repair related to bioactivity, stratified microstructure, cell migration and suppression of endochondral angiogenesis [20]. The key attributes of native OC tissue are generally incorporated into the biomimetic design of scaffolds, wherein calcified cartilage layer, a highly mineralized OC interface (≤ 100 microns), plays a critical role in repairing OC defects and the evolution of OA [21]. OC interface with unique composition and architecture is also essential to ensure overall function of OC scaffolds since while transferring outer forces, it would undergo 4 orders of modulus mutation and prevent lateral strains [4]. Biomimetic OC scaffolds are promising to consider the above characteristics, while advanced techniques are still in need to optimize the design process involving time-/money-consuming, iterative fabrication and assemble procedure. Biomechanical and bioactive properties of biomimetic OC scaffolds can be estimated via FE analysis, and the analysis process is further modified to match the experiment results. Based on the ISO standard of clinical implants, the relatively optimal design which ensures the regional characteristics and interface stability of OC scaffolds will be obtained from a series of FE iterative analysis.

Material design of OC scaffolds

Apart from the scaffold body which allows for cell proliferation, ECM interaction and deposition [22], the biomaterial within the scaffold also provides the significant biological clues of metabolic activity and tissue development. It has been proved that the surficial characteristics, and rigidity and composition of polymer materials substantially regulate the cell interactions with scaffolds [23, 24]. Thus, scaffold materials, especially functionalized composites, are urgently to be developed to assist the spatial specific reactions of cells within scaffolds [25]. Table 1 combs design concepts of different material combinations for constructing polymer-based OC scaffolds.

Polymer-based biomaterials

Synthetic polymer biomaterials with superior mechanical behavior, including poly lactic acid (PLLA), poly lactic co-glycolic acid (PLGA), polycaprolactone (PCL) and polyurethane (PU), are suitable for preparing macroporous OC scaffolds which enhance cell migration and the diffusion of cellular waste and nutrients. However, such macroporous OC scaffolds are not conducive to in vitro/vivo culture for regeneration of OC tissue because of the material characteristics including slow degradation rates, harmful degradation products and lack of reactive ligands and biological cues [26], and the rapid diffusion of nutrients caused by macropores under outer pressure. Hydrogel biomaterials,

Table 1 Biomaterial combinations for different types of polymer-based OC scaffolds

Types	Natural polymer matrix materials	Synthetic polymer matrix materials	Bioactive additives	Literatures
Stratified scaffolds	Cartilage layer: CS	–	Cartilage layer: HyA	[42]
	Bone layer: CS		Bone layer: HA	
	Cartilage layer: SA, CS	–	Cartilage layer: FGF-2, BMP-2, TGF-β1	[45]
	Bone layer: SA		Bone layer: HA, BMP-2	
	Interface layer: SA	Interface layer: GelMA	Interface layer: ß-TCP	[47]
	–	Interface layer: SO-BHET-based polymer	–	[49]
Gradient scaffolds	–	PEGDA	$PDMS_{star}$-MA	[50]
	Silk fibroin	–	R5	[51]
	Agarose	–	BMP-2 loaded SPION	[53]

such as polyvinyl alcohol (PVA) gel, hyaluronic acid (HyA) gel, chitosan (CS) gel [27], collagen (Col) gel and fibrin gel, display viscoelasticity and support stable chondrocyte phenotype, which avoids terminal hypertrophy and tissue mineralization. In 3D culture, the hydrogel creep promotes the spreading and osteogenic differentiation of MSCs, and the substrate stress relaxation alters cell morphology in addition to the enhanced cell spreading and proliferation [28]. In view of the intricate interactions between cells and hydrogels, it is challenging to tailor the differentiation of OC scaffolds into multiple lineages by the desirable combination of hydrogels [29]. In addition, it is another major challenge presented by clinical application of load-bearing OC scaffolds to overcome the low fracture energies/low elastic modulus of hydrogel substitutes [30]; encouragingly, the current strategies including structure-inserted hydrogels [31], high-strength hydrogels [32] and particle-enhanced hydrogels [33, 34] are potential to solve this issue.

Polymer-based nanocomposites have attracted significant attention in bone substitutes [35]. Inorganic components including hydroxyapatite (HA), tricalcium phosphate (TCP) and bioactive glass (BG) are often incorporated into calcified cartilage/subchondral bone layer as beneficial reinforcement phase. Previous studies demonstrate that the added inorganic phrase increases the roughness and osteoconductivity of polymers, which is beneficial for the formation of bone-like apatite and the regeneration of osseous tissue. For the specific case of nHA, it plays multiple roles in various polymers including the diffusion, adhesion and gene expression of cells, which responds to changes in the wettability and porosity of material surface tuned by nHA content [36]; in addition, the mechanical properties and osteoconductivity of the gelatin methacrylamide (GelMA)-based OC scaffold were proved to vary with the nHA content in calcified cartilage layer and subchondral bone layer [37]; for another, given the uneven dispersion of nHA in polymer via mechanical mixing method, the nHA-graft-PLGA composite (nHA-g-PLGA) was prepared to resemble the bone matrix by surface-initiated polymerization, fully embodying the reinforcement effect of nHA [38]. Designing growth factors in biomaterials is common to exert the functionality of bi-lineage differentiation of OC scaffolds. However, data indicate that growth factors tend to be diluted and metabolized in vivo because of a short half-life period, which gives birth to an available approach, namely polymer-wrapped growth factors slowly release bioactive signals [39]. Besides, the graphene-based nanomaterial, as a carrier which could absorb and transport a large number of biomolecules effectively, became attractive for OC scaffolds with region specific differentiation of MSCs [40].

Zonally organized design of materials

The materials associated with natural ECM components, such as CS, COL I, COL II, nHA and HyA, due to their natural binding sites with cells on material surfaces, have been extensively selected in layered design of biomimetic OC scaffolds [41]. Ariane E. Erickson used CS as the main component, respectively, combining with HyA to form the hyaline cartilage layer, and with sodium alginate (SA)/HA to form the subchondral layer (Fig. 1a). They found that the chondrocyte-like (SW-1353/MCSs) and osteoblast-like (MG63) cells cultured in different regions of the OC scaffold migrated to the interface of two layers to form a stable transition, and the elastic modulus of each layer could be tuned by bioactive components (nHA and HyA) [27]. In vivo implantation of the Col-based OC scaffold (containing HyA and HA in specific regions) further proved that the scaffold material designed with unique biological clues could direct the differentiation of host cells to produce cartilage due to the inclusion of HyA, and to produce calcified cartilage and bone due to the presence of HA [42]. Here despite adopting the continuous phase in different layers which improves the integrity of OC scaffolds [43], due to the diverse additives and morphological structures of the regional materials, the uniform infiltration between biopolymer solutions

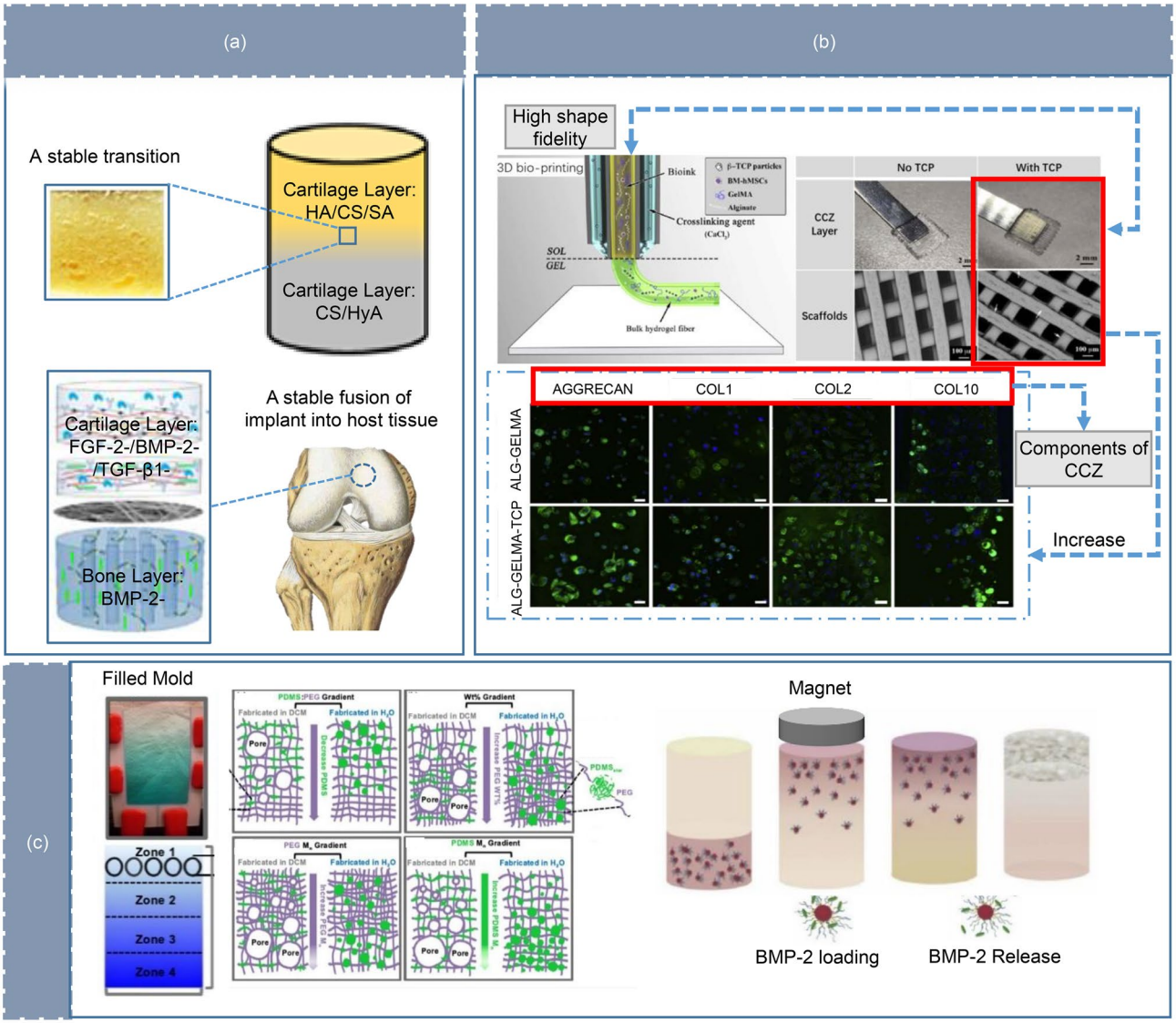

Fig. 1 Material design of OC scaffolds **a** Zonally organized design of materials: the bilayer OC scaffold with HyA and HA in specific regions (top). Reprinted from [27], Copyright 2019, Springer, and the multilayered OC scaffold with growth factors (bottom). Reprinted from [45], Copyright 2018, Elsevier; **b** material optimization of OC interface: the optimal concentration of 0.5% w/V β–TCP in GelMA/alginate bioinks. Reprinted from [47], Copyright 2019, IOP; **c** gradient design of materials: the eight gradient OC scaffolds (left). Reprinted from [50], Copyright 2013, Elsevier, and the OC scaffold with the continuous BMP-2 gradient by using magnetically aligned glycosylated SPIONs (right). Reprinted from [53], Copyright 2018, Elsevier

should be particularly noticed to sustain a stable interface. Nevertheless, little work has been devoted to the impact of solution properties and forming conditions on bridge connection between layers within the scaffold. The recent research recognizes the superior interlayer integration of OC scaffolds induced by growth factors especially in repairing large-scale OC defects since they not only accelerate the overall repair of defects but also facilitates the vascularization in subchondral layer [44]. In a case of the research on a multifunctional integrated OC scaffold (Fig. 1a): the cartilage layer consisting of the FGF-2-/BMP-2-/TGF-β1-loaded oxidized sodium alginate and N-succinyl chitosan (OSA/NCS) hydrogels; the subchondral bone layer composed of SA/nHA/BMP-2-loaded coaxial short fibers, as a result of the vascularization formation in subchondral bone layer and the sequential reconstruction of OC tissue, the combined sequential delivery strategy of the growth factors was found to support a stable fusion of implant into host OC tissue [45]. The success of this strategy lies in releasing bioactive signals to comply with the growth regulations of desired tissues, which is determined by the dose and type of growth factors as well as the loaded approaches.

Material optimization of OC interface

A sudden change between two materials may result in weak mechanical transfer and integrity in transition region [46]. Given that the collagen expression in calcified cartilage similar to hyaline cartilage and its highly mineralized bone-like nature, bi-lineage composites are presented as superior transition materials which can provide reliable interfacial connection and induce the regeneration of OC interface tissue. The 0.5% w/v β–TCP in bioinks containing 6% w/v GelMA and 4% w/v alginate was found the optimal concentration to fabricate the porous structure (Fig. 1b) which displayed potentially biological characteristics related to the development of calcified cartilage [47]. Besides biomineralization, BG particles containing copper ions (Cu^{2+}) as the dual function bioactive additive in the SA/poloxamer (F-127) substrate activated HIF pathway to improve cartilage repair and induced macrophages to shift to anti-inflammatory M2 phenotype within the Cu^{2+} concentration range of 0.5–16 ppm [48]. Another notion which attracts our attention is to explore the potential of synthetic biomaterials by simply varying the monomer ratio derived from waste/renewable materials. In this investigation, a low-cost biopolymer was developed using the aromatic ring in bis (2-hydroxy) terephthalate (BHET) as hard segment, and the long aliphatic chain in soybean oil (SO) as soft segment. Interestingly, due to the co-stimulation from the mechanical cues and degradation products of polyesters, the polyester with the 4:1 weight ratio of ESO/BHET formed the stable OC interface by simultaneously promoting the formation of bone and cartilage [49]. Here, we presume that the polyesters synthesized by the 4:1 and 5:1 weight ratios of ESO/BHET, respectively, are potential candidate biomaterials for the cartilage layer and bone layer of OC scaffolds, which is supported by the evidences of their similar swelling, degradation and different biological signals. For stratified OC scaffolds, however, the unilateral effect of such bi-lineage composite is impossible fully exploited in simple culture system, appealing for special bioreactors to obtain the required biomechanical and biochemical conditions.

Gradient design of materials

Considering the spatial variation in ECM composition and orientation from subchondral bone to cartilage, gradient design is proposed to regulate the transition properties of materials, ensuring the loading capacity and repair effects of OC scaffolds. Recently, emerging approaches by tuning spatial compositions are potential to achieve the gradients of mechanical properties and biochemical signals of OC scaffolds. Methacrylated star polydimethylsiloxane ($PDMS_{star}$-MA), a powerful component with bioactivity and osteoinductivity, was incorporated into the poly (ethylene glycol) diacrylate (PEGDA)-based hydrogel scaffolds. Four groups of continuous gradient scaffolds were prepared by varying the weight ratio of $PDMS_{star}$-MA to PEGDA macromer, the total macromer concentration, the number average molecular weight (Mn) of PEGDA and the Mn of $PDMS_{star}$-MA (Fig. 1c). Such scaffolds with tunable morphology, swelling, modulus and bioactivity had been proved to be valuable for OC tissue regeneration since they allowed for rapid screening of cell-material interactions [50]. It is worth noting that the spatially varied functions of the mentioned gradient scaffolds, which intimately relate to microphase separation of composites, are tremendously affected by solvent type and the mixing process of precursor solutions. Another novel route was proposed to form continuous gradient protein/biosilica composites for regeneration of OC tissue via in situ site-specific biomineralization. The biosilica selective peptide (R5), a bio-inspired analog derived from the silaffin peptide, can trigger and mediate the biomineralization in the hydrogel composite. The recent work revealed that the spontaneously formed gradient silicified silk/R5 (GSSR5) composite promoted the osteogenic differentiation of hMSCs in vitro in a manner consistent with the R5 gradient in the composite [51]. Some common problems exist in the mentioned methods of manually stacking materials: due to interdiffusion of solutions, the lagging cross-linking of the precursor solutions may cause the failure of the pre-designed gradient in scaffolds; and these methods are often accompanied with drawbacks of tedious procedures and inadequate versatility in other biomaterial systems. In this context, the researchers proposed a simplistic and rapid strategy to naturally form a gradient of growth factors in the hydrogel which played an important role in dictating the OC interface formation [52]. Specifically, the continuous BMP-2 gradient in the agarose hydrogel laden with hMSCs was achieved in a self-organized manner through the magnetic field effect of glycosylated super paramagnetic iron oxide nanoparticle (SPIONs) (Fig. 1c). Over a 28-day culture in an optimized OC differentiation medium, BMP-2 which orderly released from SPIONs regulated the osteogenic gene expression and tissue mineralization in the hydrogel [53]. Although the mechanism responsible for forming gradient is far from being fully understood, data have characterized the related influencing factors worthy of attention such as the SPION state in the precursor solutions and its response to magnetic force, as well as the affinity of growth factors for SPIONs; there is a necessity to emphasize another technical difficulty on how to achieve local mineralization, which may be addressed via optimizing the growth factor concentration loaded on nanoparticles.

The convention of material design of OC scaffolds is converting from independent region design to integrated material arrangement. Natural polymer materials, supporting the attachment and proliferation of osteoblasts and

chondrocytes, are prior selected to construct the unique microenvironment of bone/cartilage. Synthetic polymer materials are mainly used to tailor the processability, mechanical properties and degradation rate of scaffolds. Then, the component concentration and the additives of inorganics/cytokines/growth factors are considered to optimize the biological function of materials, including the cell response on the scaffold substrate and the compatibility with adjacent materials as well as surrounding tissues [54]. The zonally organized design of materials based on the rationale of biomimicry for tissues only needs to select the specific matrix materials optionally loaded bioactive components. However, the material design of OC interface is still a difficulty considering the regeneration and connection function of the ultra microinterface. Bi-lineage composites supporting both cartilage and subchondral bone regeneration, which provide more choices and possibilities for the design of OC interface materials, break through the impasse of simulating native OC interface. Moreover, the biological clues and mechanical gradient at interface of scaffolds are key points of material design to realize regeneration of full-thickness OC tissue. The current researches break away from designing materials for distinct tissues, instead, directly regard OC tissue as a whole part with multilayer/continuous gradient of bioactive components which flexibly alter the local characterization within the integrated OC scaffolds.

Structure design of OC scaffolds

The scaffold configuration and the intra-/extracellular signal have the certain regulatory effect on gene expression and cell differentiation within scaffolds [55]. The structure design parameters of scaffolds, such as pore size, porosity, tortuosity and interconnectivity, are generally customized to improve mechanical properties, cell distribution, phenotype of ECM protein, cell migration, nutrient transfer and formation of vascular network within scaffolds [31, 56, 57]. Here, structure layout schemes for different types of polymer-based OC scaffolds are summarized in Table 2.

Design prerequisites

It is well known that the intercellular/cell-biomaterial interactions and nutrient/waste transport are enhanced in the porous scaffold, whereas its inner architecture appears to be another crucial design factor to resist the concomitant decrease in mechanical properties, especially for the one with high porosity. From another point, the structure design of scaffolds to some extent determines the cell fate and tissue regeneration. For example, pore size takes effects in the metabolism, attachment, proliferation and infiltration of cells within the scaffold [58], subsequently affecting the fixation ability of the OC implant and the ingrowth and vascularization of tissue [59, 60]. More specifically, the optimal pore size that varies from 5 to 500 μm across cell types is recommended for tissue regeneration [61]; the enhanced interaction between chondrocytes is proved to reduce the structure stability and ECM synthesis; hence, the mean pore size less than 200 μm which favors pore coverage is preferable for cartilage layer with low metabolic activity [62, 63]. The differentiation of hMSCs cultured in OC scaffolds elucidated that the cells residing in the rhomboidal pores supported a better osteogenic differentiation, whereas chondrogenic differentiation was enhanced in the squared pores [64]. The research of surface structure on cell stimulation showed that the chondrocytes cultured on the nanofiber structure tended to lose their phenotype; in contrast, the osteogenic differentiation of MSCs was significantly accelerated by the nanofiber surface. Therefore, comparing with nanofiber

Table 2 Structure layout schemes for different types of polymer-based OC scaffolds

Types	Pore units	Organized patterns	Connected patterns	Literatures
Stratified scaffolds	Cartilage layer: Columnar structures with major and minor axes of 132.6 μm and 37.5 μm	Cartilage layer: Vertically aligned	Structure fusion	[69]
	Bone layer: Elliptical pores with major and minor axes of 33.6 μm and 27.4 μm	Bone layer: Randomly distributed		
	Cartilage layer: Microtubule-like structures with 10 μm pore size	Cartilage layer: Vertically aligned	Dissolution bonding	[72]
	Bone layer: Square pores with 450.5 μm fiber spacing	Bone layer: Lattice array		
	Interface layer: Cylindrical structures with pore size of 400 μm in diameter and 1000 μm in depth	Interface layer: Quadrilaterally arrayed	Mechanical interlock	[73]
Gradient scaffolds	Square pores with 200, 500, and 900 μm fiber spacing in each section	Lattice array In a step-changed manner	Structure transition	[76]
	G/D pore structure based on TPMS	Circularly arrayed In a continuous gradient manner	Structure transition	[77]

surface suitable for subchondral bone layer, smooth surface was preferred for cartilage layer [65].

Zonally organized design of structures

The aim of biomimetic OC scaffolds with layer-specific porous structures is to provide depth-dependent arrangement (horizontal/random/vertical) chondrocytes in the cartilage layer [66, 67], and to facilitate the recruitment and osteogenic differentiation of endogenous cells by macropores [68]. In details, the trilayer OC scaffold composed of the hydrogel top layer, the middle layer (the pore aspect ratio was 3.6 ± 0.6) and the biomineralized bottom layer (the pore aspect ratio was 1.3 ± 0.6) was prepared (Fig. 2a). Such scaffold cultured in chondrogenic medium avoided the migration of the exogenous cells (hMSCs: chondrocytes = 70:30) into the bottom layer. Then, the subcutaneous implantation suggested that endogenous cells were randomly distributed in the top and bottom layer, and the cells in the middle layer were arranged vertically along columnar channels. In vitro/vivo experiments demonstrated that such trilayer scaffold could improve cell distribution and promote the regeneration of OC tissue with obvious interface [69]. For such a part without any physical barrier, the independent regeneration of regional tissues lies in the mineral environment in subchondral layer and the chondrogenic preconditioning for

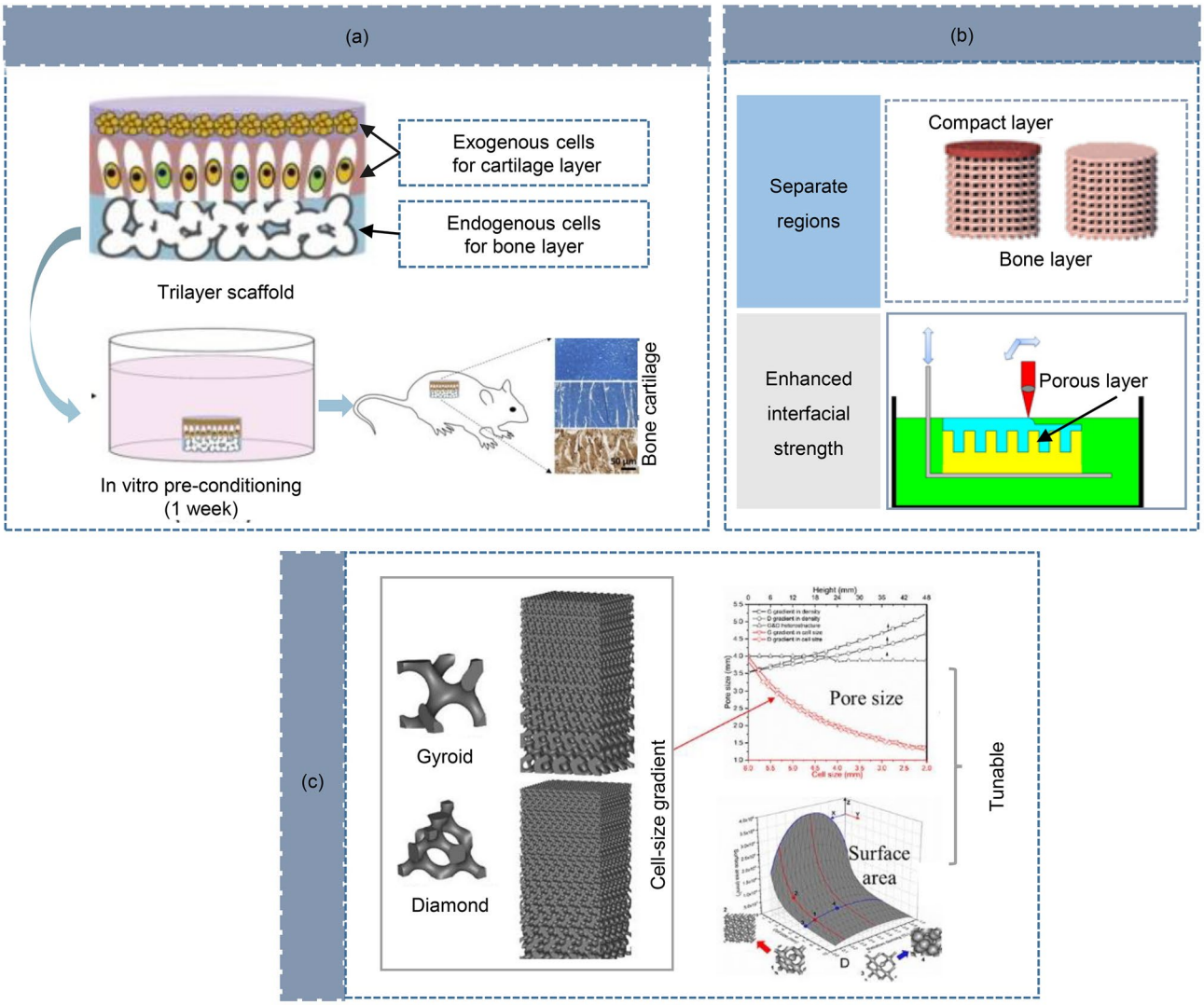

Fig. 2 Structure design of OC scaffolds. **a** Zonally organized design of structures: the trilayer scaffold composed of the hydrogel top layer, the bottom and middle layer with anisotropic macropore structures. Reprinted from [69], Copyright 2018, Elsevier; **b** optimization of interface structure: the PLGA/TCP compact interfacial layer (top). Reprinted from [72], Copyright 2018, Europe PMC, and the interfacial layer with the porous β-TCP structure (bottom). Reprinted from [73], Copyright 2015, Elsevier; **c** gradient structure design: the gradient OC scaffolds with tunable mean pore size and surface area. Reprinted from [77], Copyright 2018, Elsevier

cartilage layer, which underachieves the unique advantages of biomimetic interface in remodeling the regeneration environment of OC tissue.

Structural optimization of OC interface

The structure design of interface layer should coordinate the elastic modulus of adjacent layers to maintain the mechanical stability of OC scaffolds [70]. In addition, the couple effect of interface structure and mechanical stimulation is intimately related to the regulation of cell differentiation [71], which plays a substantial role in preventing the ossification of full-thickness cartilage [53]. The compact interface layer of PLGA/TCP composite (Fig. 2b), as an important physical barrier between cartilage layer and subchondral bone layer, provided a low oxygen tension and avascular microenvironment in cartilage layer which could induce the chondrogenic differentiation of endogenous MSCs. Surprisingly, comparing with the disordered OC interface formed in the group without a compact layer, the neo tidemark consistent with native OC interface was formed in the regenerated tissue of the scaffold with the dense interface [72]. In such an interface design protocol, however, in vitro seeding chondrocytes/cell-laden biomaterials are desired to accelerate the tissue repair due to less precursor cells in cartilage. Furthermore, the repair of OC tissue especially for tidemark formation relates to the initial integrity at interface; thus, we suppose that the interface involving the interlacing of hard and soft structures may provide a better connection between two phase materials. Inspired from the presence of gomphosis and hole-like structure upon nature subchondral bone, a series of PEG/β- TCP scaffolds with interface structures of different porosities (Fig. 2b) were prepared. The comparative analysis of these scaffolds indicated that the shear strength at interface in the 30% porosity group was nearly threefold improved compared with that in the 0% porosity group, which was in line with our previous argument. In order to promote biological bonding through in vitro ECM synthesis, the surface area of interface zone which is considered as another structure parameter to control cell behavior should also be emphasized [73]. Despite these studies, due to limited manufacturing technologies for the ultrastructure, the effect of interface structure on biochemical and biomechanical properties is not further investigated until now.

Gradient structure design

The OC scaffolds with gradient pore features aim to recapitulate the multi-level pore morphology of OC tissue, and to meet varying requirements of regional tissues on biological and mechanical properties. For example, the mechanical properties of the gradient scaffold show obvious improvement caused by the disruption of crack propagation [74]. It has also been confirmed that the pore gradient improves the cell seeding efficiency and cell distribution of scaffolds since curved channels increase the possibility of cell-scaffold contact [57]. Additionally, the cell attachment, the production of ECM, GAGs and collagen and the alkaline phosphatase activity of MSCs are increased in the gradient scaffold in comparison with one with a uniform pore size [75]. For the constantly loaded OC unit, the valuation of strain behavior of mimetic ECM is required to recapitulate its morphological evolution, thereafter providing well organized mechanotransduction for neo tissue growth. In case of the gradient OC scaffold, composed of three stacked models with 0.2 (small-pore), 0.5 (medium-pore) and 0.9 mm (large-pore) fiber spacing, respectively, the deformation behavior of the scaffold under compression was studied. The results demonstrated that the strain distribution was readily affected by the large-pore segment of the scaffold. However, little influence of additives (nHA) could be found in terms of the compressive properties and recovery behavior of the scaffold, which might be attributed to the formation of ceramic aggregates and the suboptimal biphasic interface in the particulate composite [76]. This investigation also implies that geometry and size of regional pores may work together in determining the deformation mechanism of gradient scaffolds. Based on the triply periodic minimum surfaces (TPMS) approach, the size of regional pore relevant with its geometry is controlled by the pore gradient of the porous OC scaffold (Fig. 2c). The uniaxial compressive tests showed that for the gradient OC scaffolds, the gyroid (G) structure revealed a better performance in terms of ductility and ultimate strength; and the diamond (D) structure resulted in a more uniform stress distribution due to its larger surface area and smaller mean pore size than the G structure [77]. We pay attention to the smooth and continuous structures designed by TPMS which evade the defects of lattice structures, such as straight beam-like struts and sharp turns, improving the compressive properties and fatigue endurance of gradient scaffolds [78].

The aim of biomimetic design of OC scaffolds is to provide a suitable microenvironment for the development and growth of different tissues. Firstly, the regional structure design of scaffolds is based on the relationship between cell phenotype/differentiation and design scheme including the structure and organized patterns of pore units, and the requirements of physiological functions of scaffolds. Secondly, the connection mode at OC interface is determined from the viewpoints of osteointegration and repair effect of scaffolds. So far, the structure design of OC scaffolds has been developed into two streams. The first one focuses on reconstructing the bio-inspired features of nature OC tissue, including the morphology, size and arrangement of depth-dependent collagen networks and the interlocking structure of tidemark within dense calcified cartilage. The other based on overall design concept turns to gradient OC scaffolds in

line with the hierarchical properties of nature OC tissue, which ingeniously induces the scaffold to regenerate OC tissue with desired features by biological clues. Such biological binding method of ECM synthesis which provides a bioactive and durable OC interface gives full play to the intrinsic reparative capabilities of the bone implant.

Computer-aided design of OC scaffolds by FE method

Traditional design process which involves in sequential in vitro, mechanical and in vivo tests to determine the optimal structure parameters is time-consuming and resource-intensive [79]. Thus, simulation experiments by FE method have been carried out on OC scaffolds under different load regimes to track the macroscale mechanical response of scaffolds [80–83], and from microlevel to predict the effects of design parameters on bone ingrowth, osteoconduction and differentiation within scaffolds [84, 85]. The verified mathematical model may predict the clinical durability and cellular environments of candidate OC scaffolds, and the main data obtained from a sensitive analysis provide a significant reference for optimizing OC scaffolds prior to their fabrication. The following sections will introduce the current researches of comprehensive evaluation of OC scaffolds by FE method from mechanical properties to biological activity.

The fusion capability of implants into host tissue relates to the mechanical microenvironment within scaffolds, which requires the scaffold during in vivo culture to ensure the adequate mechanical stability at interface (decreased by inferior material properties and lack of integration). Adhesives are commonly applied to fix the bone scaffolds in clinic, while the loose movement of bone implant in joint space caused by adhesive failure may lead to unsatisfactory clinical results. The FE model of the OC scaffold was established in the bone defect, and the cohesive zone model (CZM) was used to simulate the failure process of fibrin adhesive under load. The simulation results indicated that the shear displacement at cohesive interface acted as the main delamination mechanism of the scaffold, and the stronger/more flexible adhesive than fibrin could prevent the delamination of the scaffold in knee joint. Here, FE method could be used to improve biological adhesives and the experimental scheme of interface mechanical properties [81]. Inspired from nature OC tissue wherein collagen fibers penetrate from calcified cartilage to hyaline cartilage, the collagen network was integrated into the bilayer soft—stiff PEG hydrogel to rebuild OC interface of the scaffolds. The FE simulations of unconstrained compression of the OC scaffolds (Fig. 3a) indicated that comparing with the single-phase scaffold, the inserted collagen network improved the stress and strain distribution and mechanical properties (compression modulus and toughness) of the multi-phase scaffold by resisting the lateral expansion [82]. For such reinforced OC scaffolds, it is a challenge to establish constitutive models to describe depth-dependent properties and compression nonlinearity of composites, which is crucial to the failure mechanism and biomimetic design of OC scaffolds. Overall, since the mechanical evaluation at interface region is limited by experimental setups, FE is recommended to be a powerful approach to analyze the mechanical stability at interface of the scaffold under typically physiological loads.

Using FE method to optimize the deformation mechanism of the gradient scaffolds is expected to tolerate physiological loads and obtain desired mechanical responses [86]. The effects of porosity and pore shape on the compressive mechanical properties of gradient OC scaffolds in elastic stage were investigated by using FE analysis. The correlation between the scaffold porosity and its elastic modulus suggested that the 60% porosity acted as a critical value to separate subchondral bone and cartilage scaffold. Besides, the hierarchical mechanical characteristics and anisotropy effects of scaffolds were achieved by tuning lay-down angle (from 90° to 15°), which was meaningful to match the mechanical conditions of surrounding tissues [75]. In order to explore the influence of porosity gradient and pore geometry on the failure mechanism and the compression deformation of scaffolds, the gradient OC scaffolds designed by TPMS method (Fig. 3b) were also studied by FE analysis. It was demonstrated that the Z-direction gradient pattern led to a brittle-like failure at a low strain, while the radial gradient pattern caused a progressive ductile failure; moreover, compared with the bending dominated architectures (D surfaces) mainly with the shear failure of the support plate, the stretching dominated architectures (I-WP and P surfaces) possessed high bearing capacity as the amount of material contributed in axial deformation and buckling at high deformations [83]. Despite these achievements, considering material components and AM process parameters (extrusion temperature, feed rate, etc.), the process-induced microstructures and mechanical anisotropy of additive manufactured parts which highly depend on deposition direction [87] should be further included in structural optimization of load-bearing bone scaffolds.

With the in-depth study of mechanoregulation theories, FE analysis has been gradually applied in design of OC scaffolds to evaluate the regeneration ability of scaffolds. This method can explain how the internal structure affects stress and strain distribution, and based on the results predict the local tissue development within the OC scaffold [88, 89]. Since the initial stimulation for cell differentiation comes from surface strain rather than volume strain [90], the differentiation results of the scaffolds were predicted according to the following criteria: $S = \frac{\gamma}{a} + \frac{\tau}{b}$, $0 \le S < 0.001$ for resorption, $0.001 \le S < 1$ for bone, $1 \le S < 3$ for cartilage, $3 \le S < 6$ for fibrous tissue and $S \ge 6$ for necrosis, where S

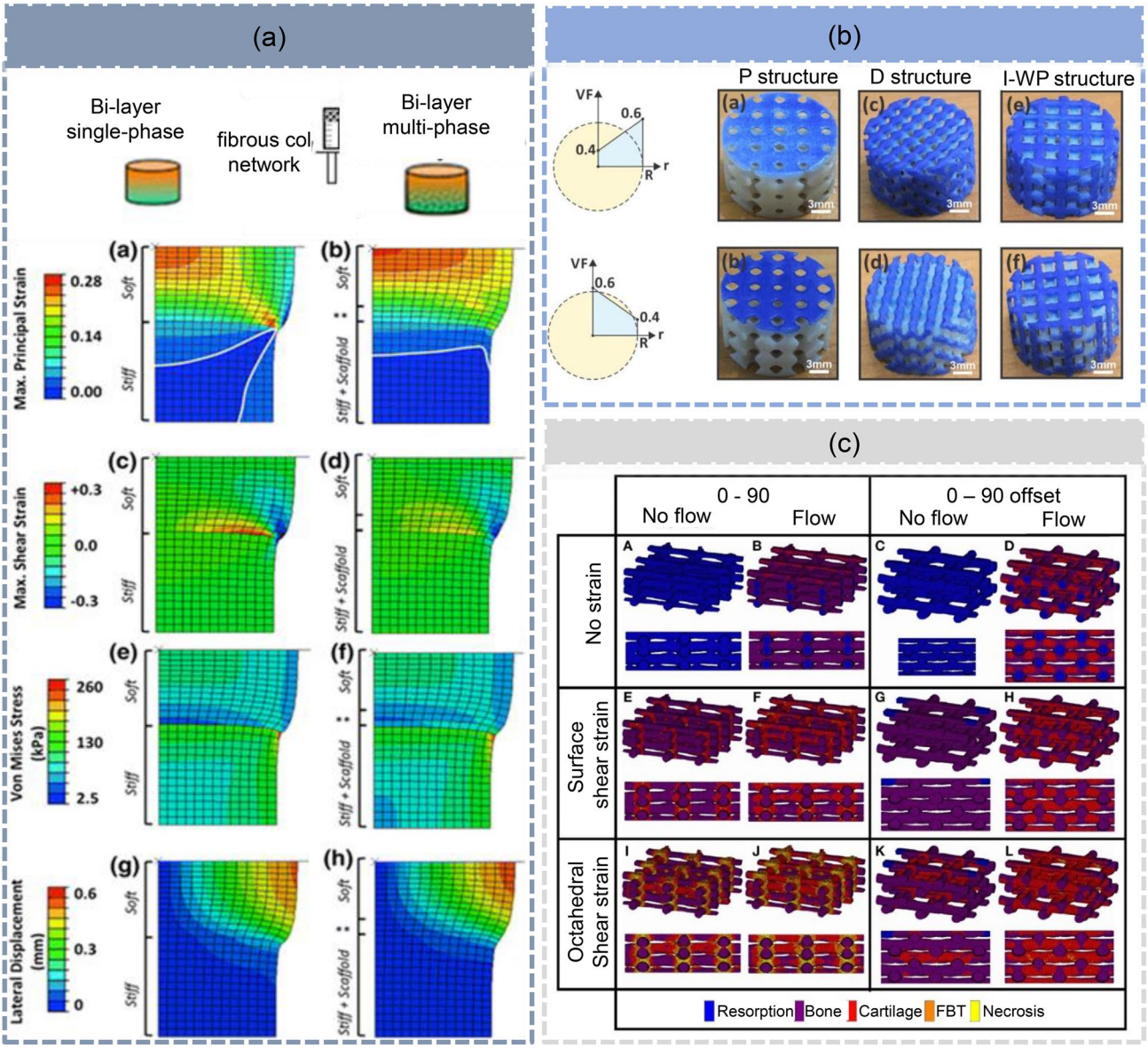

Fig. 3 Computer-aided design of OC scaffolds by FE method. **a** Mechanical properties of interface: the single-phase scaffold constituted by hard hydrogel and soft hydrogel, and multi-phase OC scaffold fabricated by inserting the fibrous network at the hard-soft hydrogel interface (top), and the FE results for the single-phase and the multi-phase scaffold (bottom). Reprinted from [82], Copyright 2015, Springer; **b** mechanical properties of scaffolds: the radially graded structures of OC scaffolds. Reprinted from [83], Copyright 2018, Elsevier; **c** biological activities of scaffolds: the cell differentiation from the FE results for the 0/90 (left) and 0/90 offset (right) structures of OC scaffolds under a fluid flow of 100 μm/s and a 10% compression strain. Reprinted from [85], Copyright 2017, Europe PMC

(the stimulus value for cells) was calculated on the basis of the FE analysis of mechanical compression and fluid dynamics (CFD), τ is fluid shear stress, γ is surface shear strain, a and b are constants of 0.0375 and 0.010, respectively, as reported in literature [91, 92]. Figure 3c shows that the distribution of fluid shear stress was mainly influenced by the pore shape and size of the scaffolds, and the strain distribution depended on whether supportive columns existed or not within the scaffolds. Additionally, as the main contributor instructing cell differentiation, the compression strain magnitude in the 0/90 geometry was greater than that in the 0/90 offset geometry [85]. Ideal OC scaffolds under outer forces should take advantage of mechanical stimulus for cells to form target tissues in addition to providing a supportive structure. Here, FE method is recommended to evaluate the biological activities of OC scaffolds which provide the basis for the bioreactor research and the optimization of scaffolds. Notably, under the conjunction of body fluid

flow and physiological activities, in order to understand the dynamic mechanical response and biological functionalities of intricate OC scaffolds, it is necessary to develop a coupled fluid–solid FE model which precisely predicts the effect of compression-induced fluid flow.

Taken together, the following design criteria are worthy of attention while designing biomimetic OC scaffolds. (1) the microenvironment design: the physicochemical properties of the matrix material can provide sites for cell adhesion and initiate interactions with cells; the micropores can promote nutrient delivery and waste metabolism within scaffolds; the geometry/orientation of the macropores can promote cell growth and differentiation, the growth of vessels into the subchondral layer and the lateral fusion of implants into surrounding tissues, (2) the scaffold design: the degradation rate of the scaffold can match the counter tissue growth; the swelling characteristics/mechanical properties at interface of two phases are compatible; the mechanical/biological properties of scaffolds is similar to host tissue. Moreover, the design trend of biomimetic OC scaffolds focuses on the anatomic structure of OC tissue mainly including (1) the biomimetic OC interface which considers the anchoring structure of tidemark and dense calcified cartilage—the ultrastructure which transfers the interface stress and induces the regeneration of OC interface, (2) the graded/continuous gradient scaffold (microstructures and components) abiding by the hierarchy of OC tissue. The design process of multifunction OC scaffolds is shown in Fig. 4.

Fabricating strategies of biomimetic OC scaffolds

The fabricating strategies of OC scaffolds have been rapidly developed to ensure the stability, quality and function of scaffolds in complex physiological environment. Traditional preparation strategies start from the chondrocyte-induced method which seeds high-density chondrocytes/chondroblasts above the scaffold for subsequent in vitro culture/in vivo implantation [93]. Thereafter, the assembly synthesis

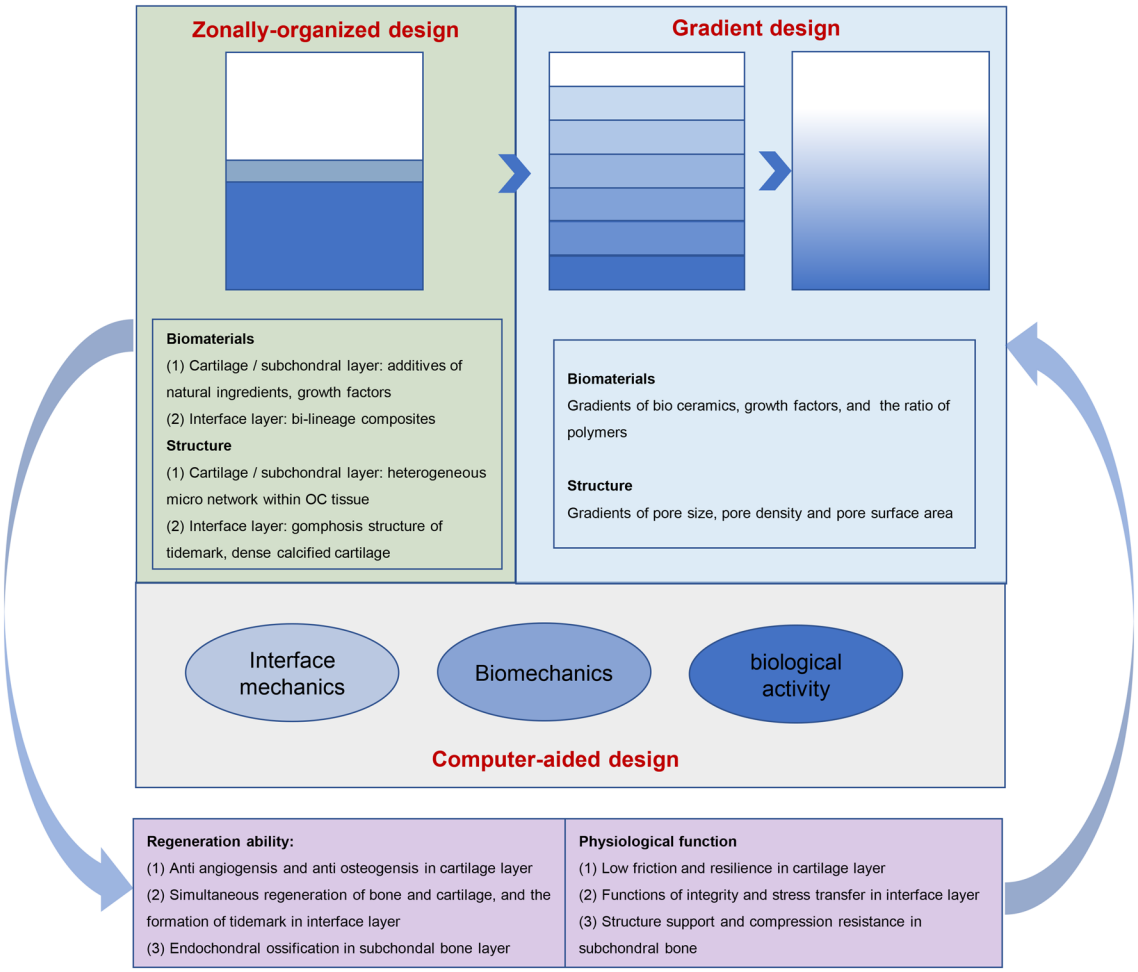

Fig. 4 The biomimetic design of multifunction OC scaffolds

method represents a turning point, attempting to provide a biomimetic ECM for cartilage regeneration. Such strategy refers to the in vitro culture of the cartilage scaffold and the subchondral bone scaffold with chondrocytes and osteoblasts, respectively, followed by assembling them into the bilayer scaffold using stitches [26] or bio glues [94, 95], etc., for further in vivo implantation. It has been pointed out that using the adhesive the brittle substrate is toughened without effecting the porous structure [94] and the cellular infiltration between layers may be inhibited [96]; however, such bonding hardly provides cohesion strength comparable to that by suture bonding [81]. It is urgent to address the severe problems caused by traditional preparation strategies: the chondrocyte-induced OC scaffolds lack layered structures to mimic heterogeneous OC tissue and cannot prevent osteoblasts from migrating into cartilage layer; the assembly synthesis method without an adequate ability to integrate biphasic scaffolds easily leads to in vivo collapse/stratification of the implants during natural degradation [97, 98].

Preparation of OC scaffolds by AM technologies

AM technologies with simple process steps and advantages in manufacturing lamellar structures have greatly innovated the traditional strategies in OC tissue engineering [39]. Furthermore, AM technologies which provide controllable process parameters, such as strand size (SZ), strand spacing (SS) and strand orientation (SO), as well as versatile pore geometry, 100% pore connectivity and reproducibility, are indeed suitable for the preparation of high-precision OC scaffolds to replicate the anatomic structure of OC tissue [99]. Although AM technologies have spawned a variety of bone scaffolds and innovative approaches in OC tissue engineering (Table 3), it remains a challenge to form OC scaffolds with gradient microstructures/multiple biomaterials including polymers, hydrogels and composites. In this chapter, we will review the current achievements of AM technologies in OC tissue engineering.

Powder-based AM technologies

The technologies in powder-based AM system for various materials from polymers to ceramics, metals and compounds of materials above are presented as a potent access to tailor-made product portfolio [100]. The process of 3D printing (3DP) is performed under ordinary temperature for preparing the gradient structure by dispensing the powder raw material of each layer and consolidating materials using a special bio-glue. However, selective laser sintering (SLS) which employs laser beam to selectively sinter powders is a more common technique to develop well-designed, stratified gradient scaffolds. The recent study used SLS technique to form the multilayer OC scaffold made of PCL microspheres and HA/PCL composite microspheres (Fig. 5a). The HA gradient from 0 to 30 wt% in seven layers of the scaffold was achieved by manually controlling the powder component supplied for each layer [101]. It is worth noting that sintering parameters for different microspheres need to be optimized to guarantee the similar thickness and structure fidelity of each printing layer; next, unsintered microspheres may be left in complicated inner pores due to unsatisfactory powder removal technique; more importantly, such technique causes lots of material internal flaws which dramatically undermine the elastic modulus of composite scaffolds, comparing with another powder-based AM technology described below. The dual (porosity and material) gradient HA/PCL OC scaffolds were developed by a multi-material extrusion 3D printing system (Fig. 5b) where the powder mixtures in metal cartridges were heated at 160 °C and then extruded through a 22G blunt tip needle. The dual gradient scaffold was printed with the additional step of switching materials for each stacked section of the scaffold [76]. Despite these studies, further investigation of manufacturing process is needed to address following issues: it is impossible to form the continuous material gradient by manually switching powder mixtures; additionally, the melt bonding of segmented depositions particularly for varied components readily forms failure points at interface between layers.

Table 3 AM technologies for preparing polymer-based OC scaffolds

AM technologies	Raw materials	Supporting material	Solidification conditions	Extra heat	Material switch	Literatures
SLS	PCL, HA	Yes	Ordinary temperature	Laser	Manual control	[101]
FDM	PCL, HA	No	Ordinary temperature	160 °C	Manual control	[76]
Extrusion 3D printing	PNAGA, β-TCP, TGF-β1	No	Ordinary temperature	70-75 °C	Manual control	[106]
Extrusion 3D printing	Alginate, GelMA, Methacrylated HyA/chondroitin sulfate, β-TCP	No	$CaCl_2$ and UV light	No	Program control	[107]
Extrusion 3D printing	Col, SA, Gellan	Yes	$CaCl_2$	No	Manual control	[111]
SL	GelMA, PEGDA, nHA, TGF-β1 PLGA	No	UV light	No	Manual control	[39]
SL	PEGDA, β-TCP	No	UV light	No	Program control	[114]

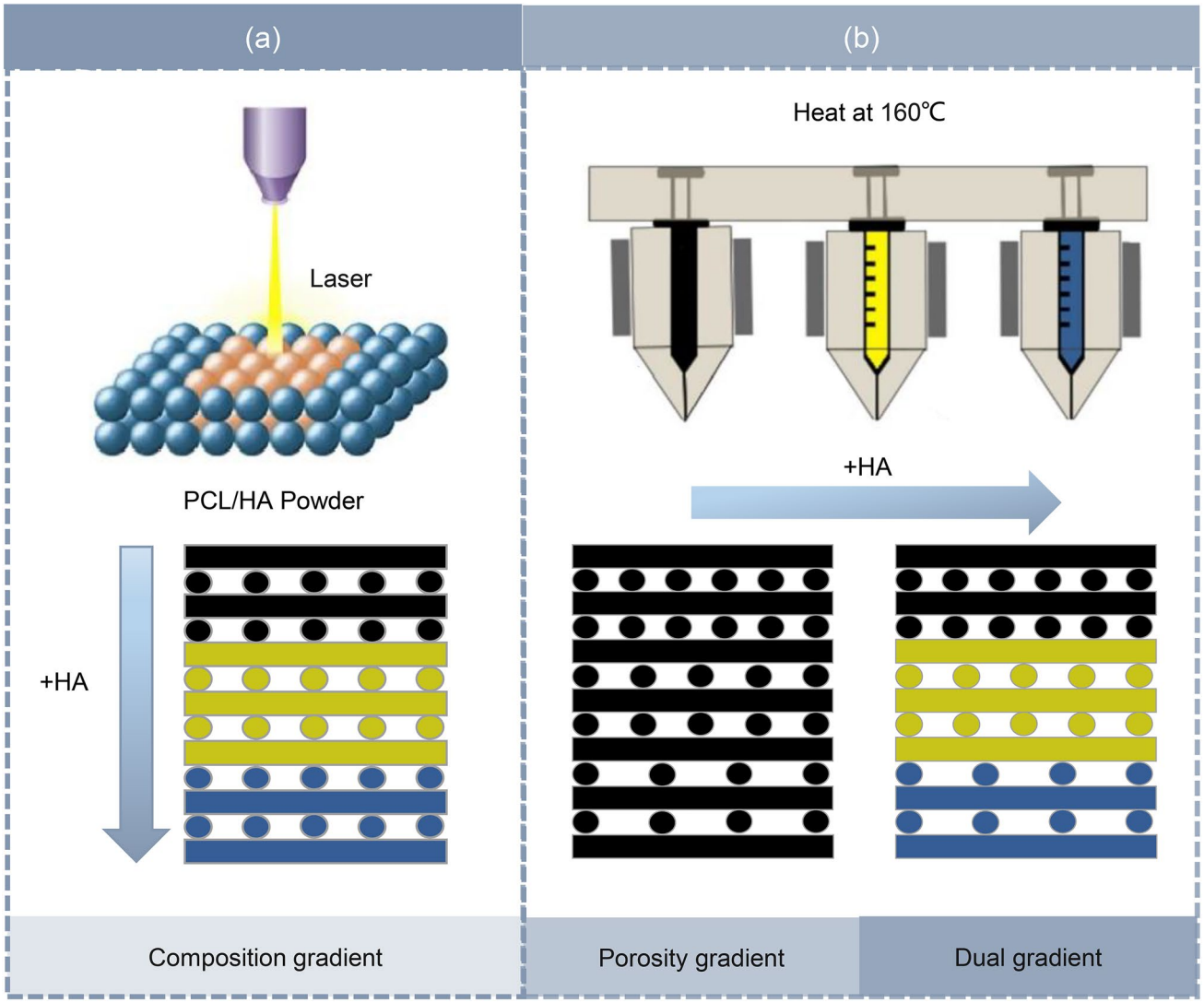

Fig. 5 Powder-based AM technologies for preparing the PCL/HA gradient OC scaffolds. **a** SLS: the multilayer OC scaffold with HA gradient. Reprinted from [101], Copyright 2017, Europe PMC; **b** extrusion printing: the porosity/dual (porosity and HA) gradient OC scaffolds. Reprinted from [76], Copyright 2019, Elsevier

Hydrogel-based AM technologies

Biopolymer hydrogels have been widespread utilized to reproduce ECM of OC tissue since by extrusion 3D bioprinting, hydrogels can be flexible controlled to tailor the biochemical and mechanical properties of complicated scaffolds whilst maintaining high viability of cells encapsulated in bioinks. The bioink viscosity which can be altered by adjusting the bioink component [102] /the tackifier content [103] and pre-cross-linking [104], etc., plays an important role in the printing process. To eliminate the impact of high viscosity on injectability, thermoresponsive hydrogels [105] are presented as potential bioinks to prepare robust scaffolds. In a study, the poly (N-acryloyl glycinamide) (PNAGA)-based thermoresponsive hydrogel was developed to prepare the gradient OC scaffold by thermal-assisted extrusion 3D printing (Fig. 6a). In this printing process, the hydrogel in a flowing sol state caused by heat was continuously extruded and immediately formed gel after deposition on the cooled substrate. The bioactive molecules, including TGF-β1 growth factors in the top layer and β-TCP particles in the bottom layer, respectively, were precisely controlled by the program to alternately perform printing [106]. Microfluidic printing was presented to avoid the incongruous mechanical and swelling properties of biphasic OC scaffolds. Specifically, such technique could allow rapid mixing/switching among two bioinks by programming the microfluidic pumps without effecting cell viability. Thus, the heterogeneous structure of OC tissue could be realized by depositing continuous gradient biological, chemical and mechanical

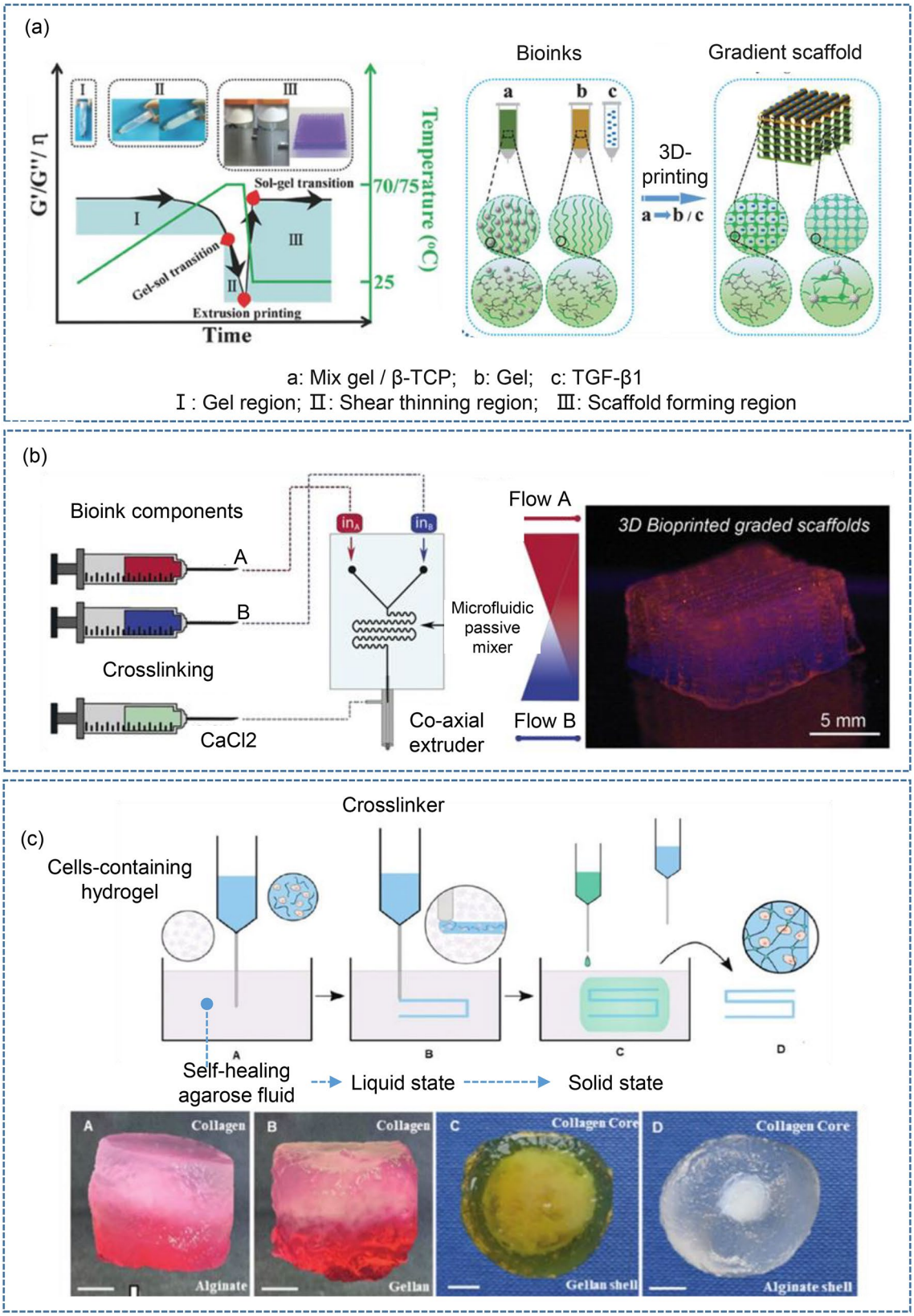

Fig. 6 Hydrogel-based AM technologies for preparing OC scaffolds. **a** Thermal-assisted extrusion printing: the high-strength PNAGA-based gradient OC scaffold. Reprinted from [106], Copyright 2018, Wiley; **b** microfluidic printing: the OC scaffold with a continuous gradient interface. Reprinted from [107], Copyright 2019, Web of Science; **c** suspended layer additive manufacture: the biphasic OC scaffolds with high shape fidelity. Reprinted from [111], Copyright 2019, Wiley

cues(Fig. 6b) [107]. Here, we suppose that it is worthy of attention to the mixing performance of high viscous hydrogels in microfluidic systems, and the double cross-linking for low viscous polymeric solutions to guarantee the fidelity and high strength of printed structures. Another extrusion 3D printing for low viscosity bioinks, namely the embedded printing, can temporarily maintain the hydrogel shape deposited in the self-supporting materials including viscous liquids, particulate gels and solid gels [108–110]. Based on this method, the biphasic OC scaffolds (Fig. 6c) were produced by extruding low viscosity bioinks into a self-healing agarose fluid-gel matrix. Such fluid-gel matrix exhibited a solid state at low shear, while it would turn to a liquid state under stress and recover viscoelasticity quickly after the removal of stress. Thus, the deposited bioinks were suspended in such matrix to prevent the collapse of the printed structure. Surprisingly, the porosity gradient at interfacial region which was formed between distinct hydrogels via natural interlayer fusion enhanced the integrity of OC tissue through biological induction [111]. Overall, the process details of such technique such as the impact of fluid-gel matrix on structure distortion and suspending capacity, and the diffusion rate of bioinks and cross-linker on printing resolution, etc., are far from being fully understood.

Hydrogel-based extrusion 3D printing combined with other technologies (freeze-drying, temperature-assisted, photocuring) is flexible enough to assist in shaping various polymers. In details, the viscosity and rheological properties of hydrogels need to be optimized via altering ingredients/outer conditions to achieve controllable, uninterrupted flow of bioinks, and to maintain the high fidelity of the printed structure. Then, cell-loaded bioinks should possess weak gel properties to undergo the shear forces during the extruding process and prevent the cell sedimentation in the syringe [47]. To preserve cell viability in suitable hydrogel characteristics, recent researches focus on the depositing and forming conditions of bioinks. For example, the side effects of extra heat, photoinitiator toxicity, curing period, UV light density and shear stress (regarding to printing pressure, bioink viscosity and nozzle diameter) on cell viability should be taken into account.

Liquid-based AM technologies

Stereolithography printing (SL) is another AM technology for forming OC scaffolds by curing liquid resin bioinks layer by layer under the UV light. Researchers can directly adjust the component ratio of functional nanocomposites/bioactive molecules and curable bioinks to produce uniform/non-uniform bone scaffolds [37, 112, 113]. For example, the core–shell TGF-β1 PLGA nanoparticles were prepared by coaxial electrospraying method, and the curable bioinks of GelMA/PEGDA/nHA and GelMA/PEGDA/TGF-β1 PLGA were printed in different regions through SL technology to manufacture the biomimetic OC scaffold (Fig. 7a). It is worth mentioning that the 28-day slow release of TGF-β1 growth factors encapsulated in nanoparticles could continuously increase the expression of chondrogenic gene in the cartilage layer without effecting the osteogenic differentiation of hMSCs in the subchondral layer [39]. It is well known that the part being constructed by traditional top-down SL printing is fully immersed in the liquid matrix, which exists problems like material waste and residual clean; besides, for the fabrication of large parts with intricate components, an automatic material switching apparatus along with relevant algorithms is highly anticipated. A customized prototype multi-material SL system based on bottom-up mask projection was developed to address these problems. In this system, the material switching and cleaning were simultaneously achieved by rotating the three-section vat, and curing characteristics of different materials were matched by controlling exposure to ensure the overall accuracy of multi-material fabrication. In a case, the biphasic OC scaffold prepared by this technology using PEGDA hydrogel and β-TCP ceramic suspension showed considerable interfacial strength which was realized by altering exposure parameters and process sequence(Fig. 7b). This printing system with high accuracy was proved very suitable for manufacturing OC scaffolds with a complex transition interface/inner structure [114]. It is noted that in consideration of residual in sponge accumulated by material switching, it is not recommended to real-time alter the material composition particularly for high viscosity composites using the multi-section vat. These researches present some other limitations of SL techniques applied in BTE: the error of curing effect caused by the scattering and reflection of UV light cannot be eliminated based on empirical work; moreover, the toxicity of photoinitiator/dispersant used in the printing process may produce some effects on cell viability.

Preparation of OC scaffolds by multiple technologies

The limited factors, such as system complexity, process conditions, possible design resources and available materials, make single process not ideal for preparing physiological full-thickness OC scaffold. To increase the diversity of OC scaffolds, other techniques have been introduced into emerging AM-based strategies [55]: (1) superposition of multi-layer structures, (2) combination of porous structures and hydrogels and (3) hydrogels embedded with nanoparticles. Table 4 shows the main characteristics of different strategies for preparing biomimetic polymer-based OC scaffolds by multiple technologies.

The regional customization of biphasic OC scaffolds can be realized by selecting the appropriate technology

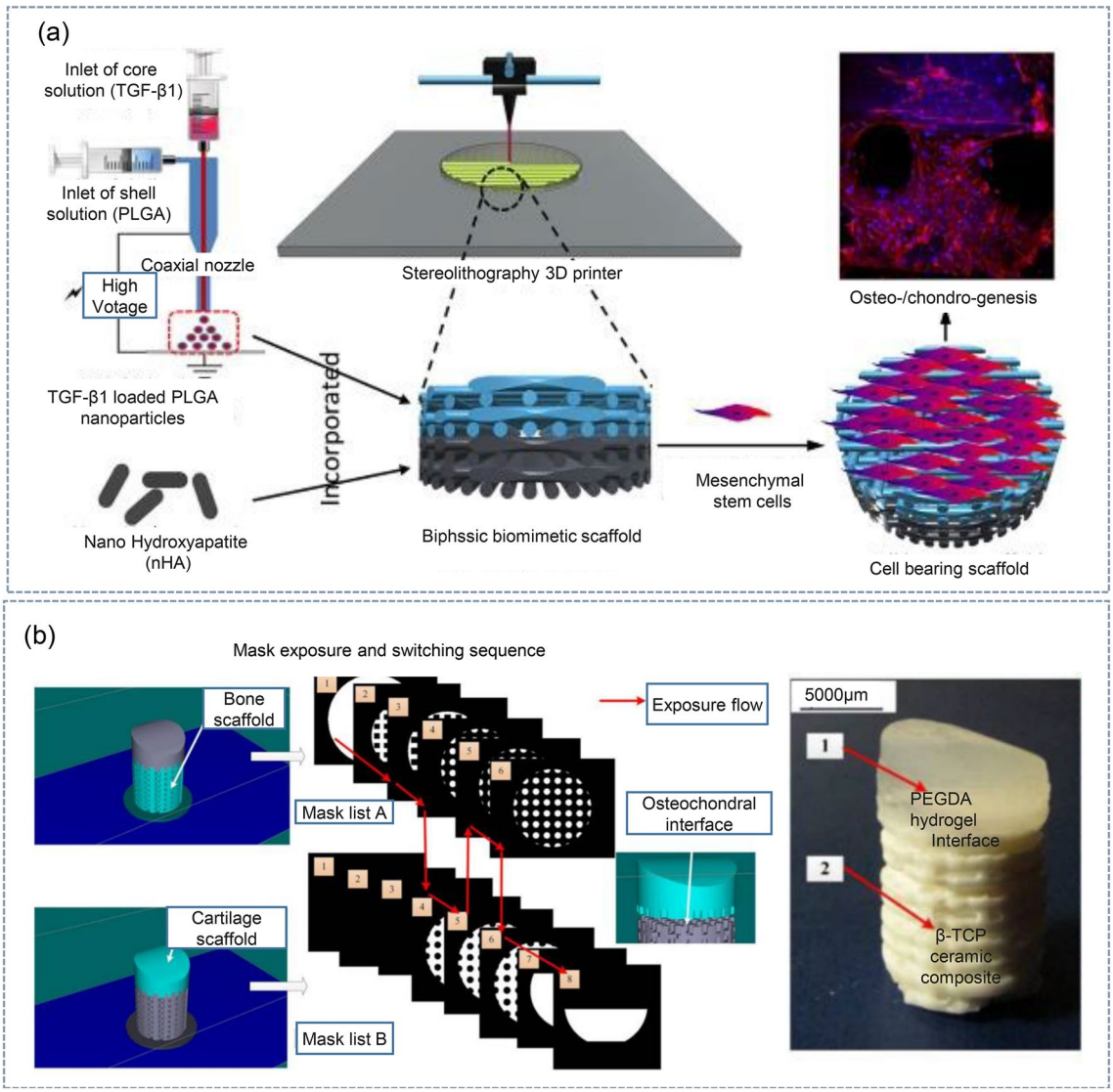

Fig. 7 Liquid resin-based AM technologies for preparing OC scaffolds. **a** The biphasic OC scaffold with HA in the subchondral layer and TGF-β1 in the cartilage layer. Reprinted from [39], Copyright 2019, NCBI; **b** the biphasic OC scaffold with a ultrastructure at interface. Reprinted from [114], Copyright 2019, Emerald

according to the material characteristics. Zhengyu Li synthesized the calcified cartilage layer and subchondral bone layer by extrusion 3D printing technology by which β-TCP particles were mixed into PLGA solution dissolved in 1,4-dioxane, and the mixed solution was immediately solidified after being ejected onto the − 30 °C workbench surface; the cartilage layer was prepared by thermally induced crystallization (TIC) technology which promoted the formation of columnar crystals of cartilage matrix along the direction of vertical temperature gradient; finally, the surfaces of the two layers were slightly dissolved in spay drops of 1,4-dioxane to assemble the OC scaffold (Fig. 8) [105]. In another study, by introducing N-acryloyl 2-glycine (ACG) reversible hydrogen bond into GelMA hydrogel system, the integrated high-strength OC scaffold was prepared to provide the mechanical support for the early stage of OC repair (Fig. 9). Specifically, the bioink B of PACG10-GelMA10 hydrogel loaded with manganese ions (Mn2+) for the cartilage layer and the bioink A of PACG35-GelMA7 hydrogel loaded with BG for the subchondral bone layer were precisely tailored by thermal-assisted extrusion printing. The main hydrogen bonding interacted in PACG-GelMA network at -10 °C workbench, followed by UV light to initiate covalent cross-linking to further fix the scaffold [115]. Importantly, the combination of double cross-linking and integrated manufacturing process provides the continuous and robust PACG-GelMA structure, avoiding the delamination and collapse of stratified scaffolds upon contacting body

Table 4 Different biomimetic polymer-based OC scaffolds prepared by multiple technologies

Categories	Strategies	Materials	Characteristics	References
Superposition of multilayer structures	Extrusion printing + TIC	Cartilage layer: Cartilage matrix	The calcified layer synthesized by extrusion printing separated the bone and cartilage areas, providing the stable microenvironments	[105]
		Bone layer: PLGA, TCP	The directional cartilage layer constructed by TIC technology was similar to the anatomic structure of nature cartilage	
Superposition of multilayer structures	Extrusion 3D printing + photocuring	Cartilage layer: PACG-GelMA, Mn^{2+}	The bioactive substances (Mn^{2+} and BG) were precisely tailored in the hydrogel scaffold by extrusion 3D printing	[115]
		Bone layer: PACG-GelMA, BG	The GelMA polymerization was initiated under UV light, and the main hydrogen bonding in the PACG-GelMA network was interacted at -10 °C to fix the formed scaffold	
Combination of porous structures and hydrogels	FDM + dip-coating method	Hydrogel: FEFEFKFK	The FEFEFKFK coated on the PCL lattice improved the microenvironment for ECM deposition	[116]
		Lattice: PCL	The PCL lattice increased the overall rigidity of the OC scaffold	
Combination of porous structures and hydrogels	FDM + extrusion 3D printing + photocuring + inkjet printing	Hydrogel: GelMA, Pluronic	The different cell populations were regionally deposited into the PCL framework by multiple technologies	[117]
		Lattice: PCL	The microchamber system reinforced hydrogel orientated spheroid growth and its fusion to host tissue	
Hydrogels embedded with nanoparticles	FDM + casting process + photocuring	Hydrogel: PEG, PEGDA	The macroporous structure of the hydrogel OC scaffold was indirectly controlled by FDM	[67, 74]
		Leachable mold: HIPS	The distribution of nHA and growth factors of the scaffold was tailored by casting process, promoting biphasic differentiation of the scaffold	

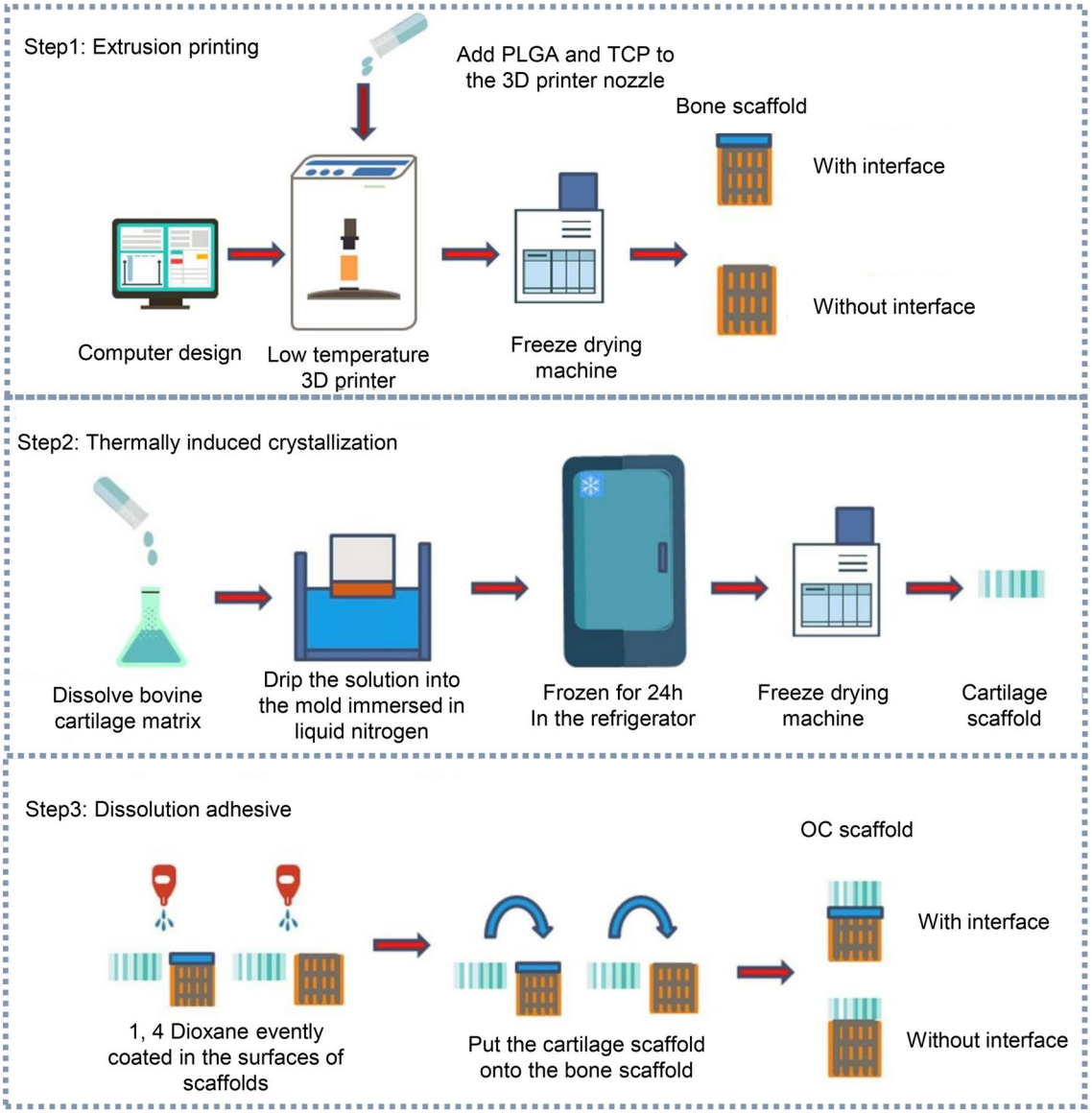

Fig. 8 Superposition of multilayer structures. The schematic of preparing the OC scaffold by three steps. Reprinted from [105], Copyright 2018, Elsevier

liquid. However, this printing system cannot support for cell-loaded bioinks due to the introduction of small molecular ACG monomer.

Other approaches have focus on the development of porous structure reinforced hydrogels through multiple technologies. In such strategy, the stiff phase provides a template for ECM-like hydrogels and an initial mechanical support for OC tissue regeneration; and the soft hydrogel is desired to enhance ECM deposition and exhibit controllable mechanical properties. For example, the β-sheet self-assembling peptide hydrogel (SAPH) FEFEFKFK (F, phenylalanine; E, glutamic acid; K, lysine), an ideal cell culture system which initiates gelation easily and induces differentiation without stimulation, was successful coated onto the FDM porous PCL structure by dip-coating method (Fig. 10a). The hydrophilicity of the OC scaffold was improved by its internal filled hydrogel, and the FEFEFKFK network around the damaged cartilage provided a suitable environment for the proliferation and differentiation of chondrocytes. After a 12-week in vivo implantation, the 3.0% SAPH-coated PCL scaffold was proved to provide a framework for ECM deposition which ensured the stable regeneration of OC tissue even with a tide mark observed [116]. Here, the hydrogel viscosity is the main point to be mentioned because the high viscosity hydrogels cannot be completely immersed in the porous structure, and low viscosity ones are rapidly lost from the structure surface. In addition, the problems caused by manual seeding of cells onto scaffold, such as uneven cell

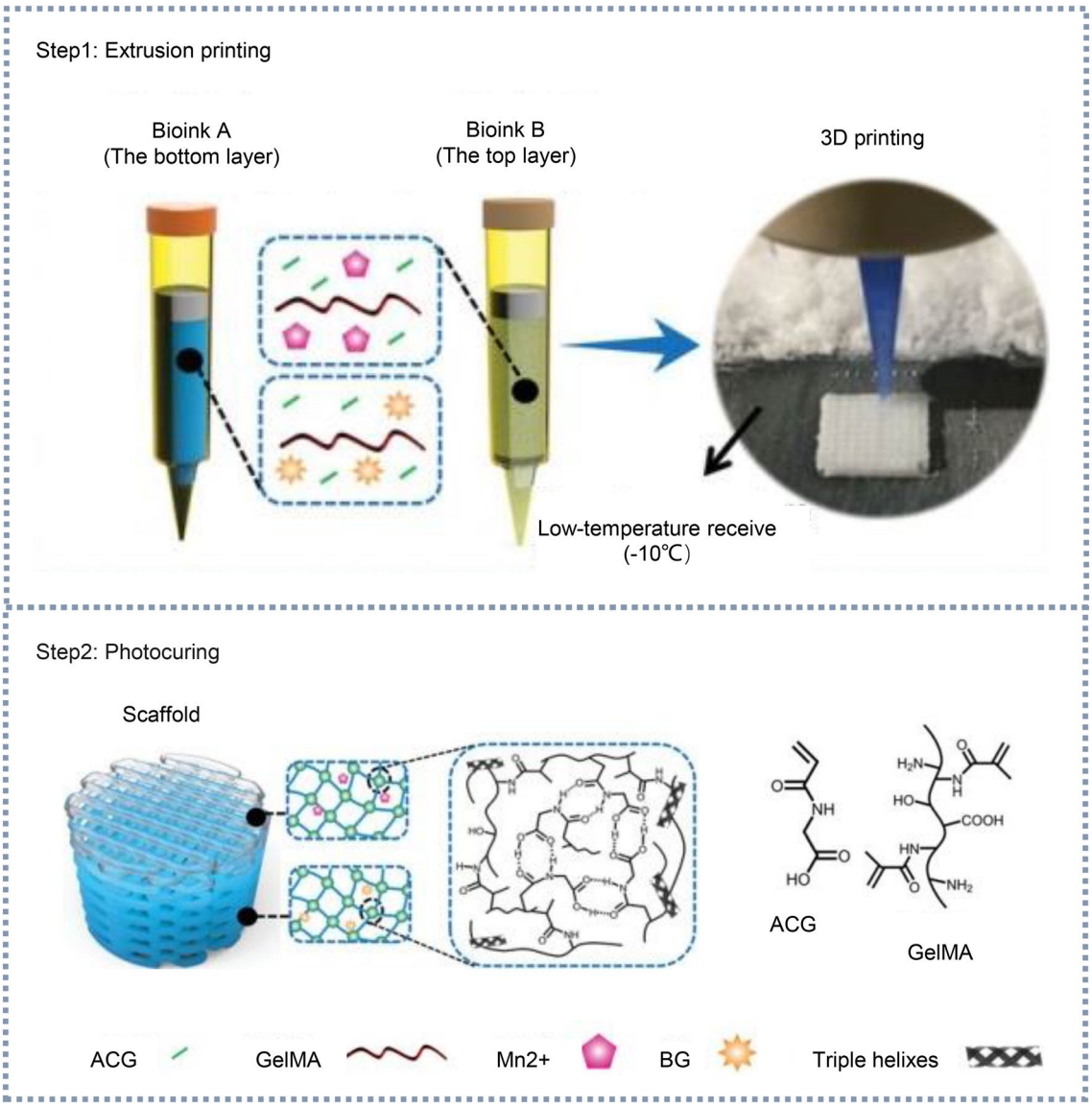

Fig. 9 Superposition of multilayer structures. The schematic of combining extruding printing with photocuring for preparing the high-strength OC scaffold. Reprinted from [115], Copyright 2019, Wiley

distribution, deficient cell–cell interaction and the obscure growth orientation of cell spheroids, may result in the failure to induce the anisotropic collagen network within the engineered OC tissue. Hence, recent researches push emerging concepts to accurately assemble cells (species, location, density) within the scaffold along the anatomic structure of nature tissue. A three step, multi-tool bioprinting approach which avoided above problems was presented to fabricate the OC scaffold (Fig. 10b). Firstly, the enhanced PCL framework including an extended microchamber system for the cartilage layer, and a porous structure for the stiff subchondral layer, was printed by fused deposition modeling (FDM) printing. Then, the MSC-loaded GelMA bioinks/the pluronic bioinks were selectively printed in alternate holes of the PCL framework. The GelMA occurred cross-linking under UV light, while microchannel network formed in the pluronic region which promoted the nutrient diffusion in the tissues during the bioreactor culture process. Finally, the array of cells (MSCs and chondrocytes) was rapidly deposited on the extended microchamber system to form the cartilage layer by inkjet printing technology [117].

The combination of casting processing and FDM printing shows its unique advantages in fabricating macroporous hydrogel OC scaffolds. The PEG/PEGDA hydrogel was cast into the FDM printed high impact polystyrene (HIPS) mold for further cross-linking under UV light; then, a highly interconnected porous structure was left after the ultrasonic treatment in D-limonene and ultrapure

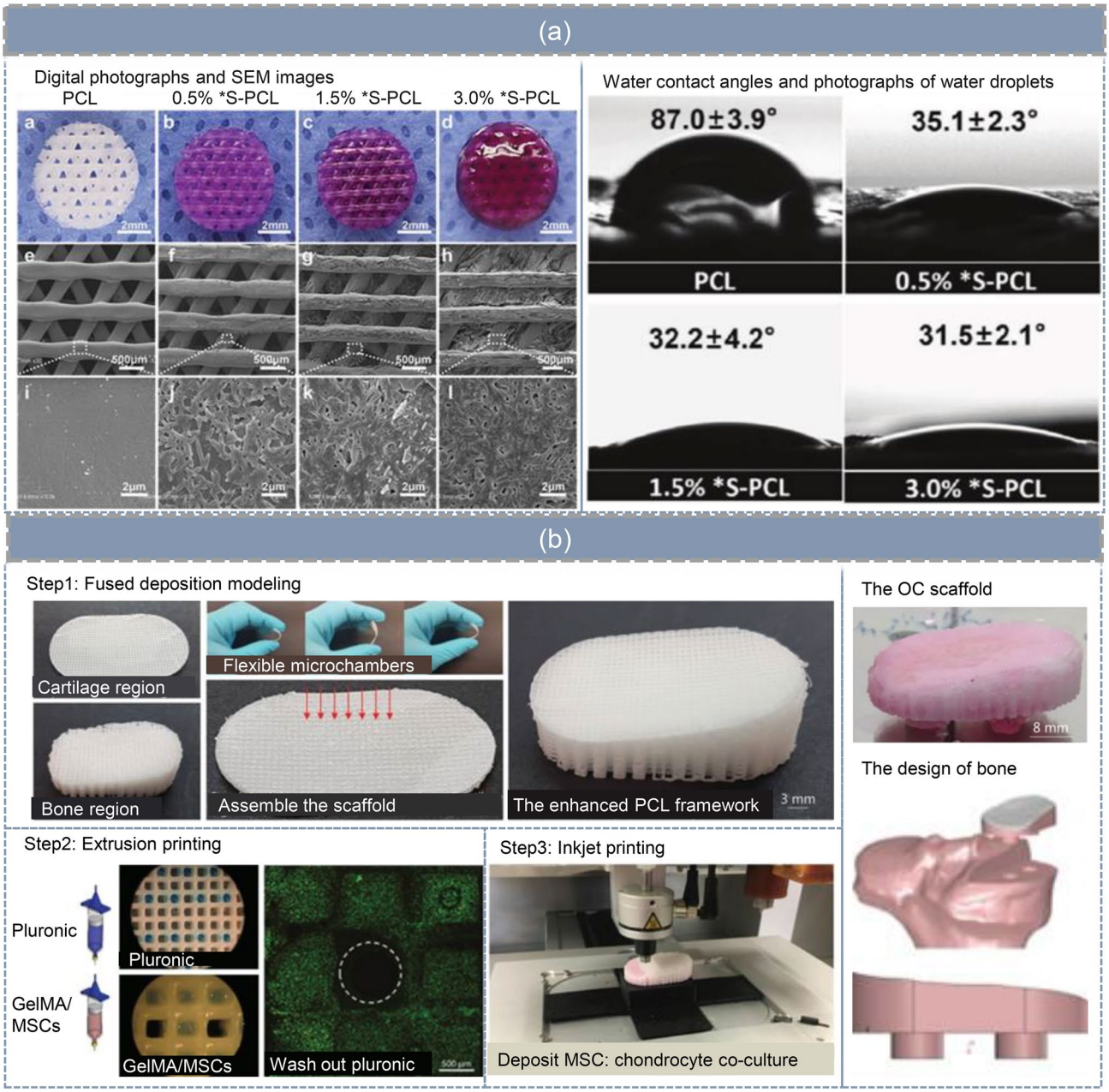

Fig. 10 Combination of porous structures and hydrogels. **a** The schematic of combining FDM with dip-coating method for preparing the PCL/SAPH OC scaffolds. Reprinted from [116], Copyright 2019, Wiley; **b** multi-tool bioprinting for preparing the OC scaffold. Reprinted from [117], Copyright 2019, Elsevier

water for dissolving the HIPS (Fig. 11) [74]. The versatility of FDM printing supported the precise pore density, distribution and alignment within the hydrogel scaffold, which was essential to improve the mechanical performance and cell behaviors of the OC scaffold. The biphasic differentiation of the OC scaffold was realized due to the incorporated nHA in the subchondral bone layer and the chondrogenic growth factors in the cartilage layer [67]. However, based on this principle, it remains a challenge to achieve continuous gradient distribution of bioactive clues for regeneration a stable OC interface; additional, the insufficient casting and mold release of the hydrogels with high HA content, and limited solvents/sacrificial molds are potential problems effecting the forming accuracy of OC scaffolds.

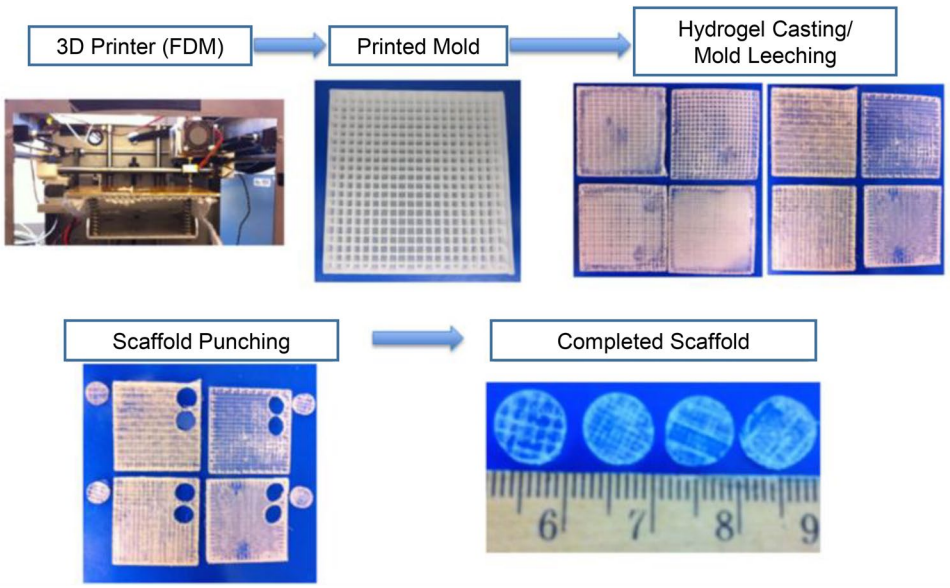

Fig. 11 Embedding of nanoparticles: the schematic of combining FDM with cast process for preparing the macroporous hydrogel OC scaffolds. Reprinted from [74], Copyright 2016, IOP

Future perspective

In the past few decades, significant progress has been made in biomaterial/structure design and processing technologies, which promotes the development of biomimetic OC scaffolds. As mentioned previously, more attention has been paid to ideal OC scaffolds in clinical application which should (1) possess compatible mechanical properties with host tissue, maintain structural integrity and stability and provide temporary physiological functions of subchondral bone and cartilage in tissue regeneration, (2) support cell metabolic activity and promote cell adhesion and proliferation and (3) induce cells to differentiate into target tissues, and exhibit the special functions of anti angiogenesis and anti-osteogenesis in cartilage layer. The following sections will present some viewpoints on future development of OC tissue engineering.

Integrated biomimetic OC scaffolds

It is a promising route to develop the integrated OC scaffold with multilayers/a gradient structure since it can reestablish cell-tissue interactions [118] and solve the problem of the assembled OC scaffolds. Moreover, the biological bonding of synthesizing ECM between chondral and osteoid tissue has gradually been considered as a promising trend to form a durable and interconnected OC interface [119]. Finally, the precise profile of the scaffold is also a crucial factor which ensures the successful implantation and effective fixation of the scaffold in the focus area. In general, the aim of integrated design of biomimetic OC scaffolds is to provide the high soft-hard interface strength, desired biomechanical properties and self-repair capacity of artificial bone grafts. We suppose that in designing biomimetic OC scaffolds, computer-aided design is far from being developed to play the best coupling effect of various design elements, which may be a difficulty to be addressed.

Novel biomaterials and technologies for fabricating biomimetic OC scaffolds

Differing from directly adding commercial ceramic particles into the polymeric matrix, in situ self-assembled technology breaks a new path for synthesizing bone nanocomposites which assure a chemical stability of the scaffold during the healing of OC tissue lesion; in addition, the low crystalline HA existed in immature bone can also be spontaneously formed through self-assembled fabrication [6]. From the strengthening and toughening mechanism of nanocomposites, the hydrogels with self-assembled CaP nanoparticles show the enhanced tensile strength and fracture energy in comparison with the counterpart obtained by physical blending method [120]. The functional nanocomposites can be formed by altering the mineralization activator and the external physical/chemical stimuli, and combined with AM technologies which offers a useful reference to achieve the personalized fabrication of OC scaffolds. Another meaningful point is that after the self-assembling of nanoparticles, the growth factors pre-designed in bioinks may be released in a controlled manner to stimulate the cell behaviors in a long term. The hydrogel without the capacity to support its own weight during extrusion bioprinting may lead to failure to obtain macroporous scaffolds. In addition, endochondral ossification guided by channels/canals can improve the osteogenic potential of subchondral layer, resulting in robust bone and better integration of the implant. In this

case, future studies may focus on sacrificial materials such as gelatin, sucrose and pluronic, etc. which can be printed in the pre-designed positions to act as temporary support materials, and form the macrocanals/mesoscale pores after washing away [121]. Despite the synchronous 3D bioprinting capable of preparing the macroporous hydrogel constructs, it is still difficult to directly develop complex architectures considering the problems of solidifying sacrificial bioinks and steadily extruding two kinds of bioinks simultaneously [122].

Standardization system of multi-material design and hybrid biological manufacture

AM technologies have attracted widely attention in the preparation of integrated OC scaffolds in that they can truly realize the gradient and personalized manufacture of scaffolds. Hybrid manufacture which overcomes the limitations of single AM technology, through launching the conversion function of multi-materials [107, 114] obtains heterogeneous OC tissue, and through precisely positioning cells in auxiliary process [117] achieves the hierarchical distribution of cells and the organization of mesenchymal condensations. In particular, it is a possible trend to develop multifunctional AM technologies for various materials which can meet the needs of integrity and individuation of OC scaffolds. For example, we suppose that the manufacturing system combined SLS with 3DP which is suitable for the forming of ceramics, synthetic polymers and their composites is worth developing to prepare OC scaffolds (Fig. 12). The main advantage of this approach is that it can quickly match the technology according to the material properties, and fully explore the potential of the two processes in printing composites. However, some problems in the integrated manufacturing process also need to be further investigated: the stable and controllable switching of bioinks; the rapid response of process parameters to biomaterials; the coordination between printability, shape fidelity and printing resolution; and the competing effects between cell/growth factor activity and printing conditions. Taken together, a simple and versatile printing system which can be applied to simultaneously produce the bone-like and cartilage-like composites is highly anticipated in future research of OC tissue engineering.

The cost-effectiveness also receives widespread attention owing to the long period and high cost for the design, manufacture and cell culture of OC scaffolds. The combination of theories on cell biology, biomaterials and bioengineering mechanics, etc., and computational simulation methods not only provides a favorable means for the design of OC scaffolds, but also explains the intrinsic relationship between the inner structure, external stimulation and biology performance of scaffolds. The general classification standard and a set of controllable design parameters can be obtained by comparative analysis of computer simulations and experiments of a series of scaffolds. Then, the high-precision manufacture of optimal OC scaffolds can be realized by manipulating the design parameters to meet patients' special needs for scaffolds and using the advantages of AM technologies. Thus, the integrated process of design and manufacture of OC scaffolds in a system of standardization, automation and

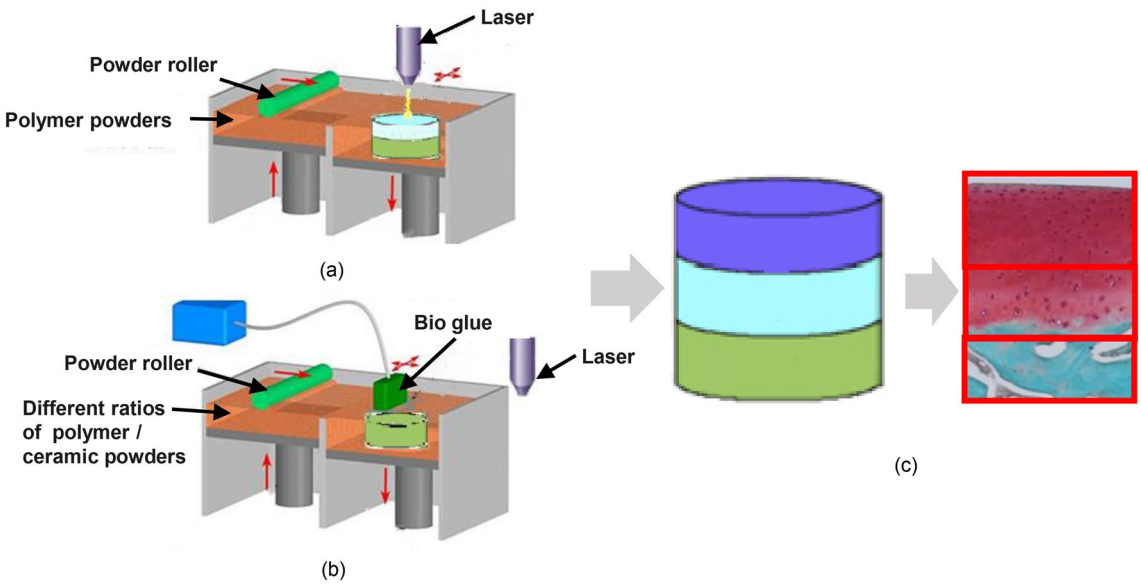

Fig. 12 The multifunctional AM technology for preparing OC scaffolds. **a** the middle (calcified cartilage) layer and the bottom (subchondral bone) layer prepared by 3DP and SLS; **b** the top (cartilage) layer prepared by SLS; **c** the integrated biomimetic OC scaffold

modularization is another trend in OC tissue engineering which pushes the clinical transformation of products.

OC tissue engineering has indeed entered an exciting time in which much work needs to be done to create ideal OC scaffolds. Fortunately, it is expected to see more positive results in the preparation of OC scaffolds with the development of AM technologies integrated with various knowledge.

Acknowledgements Funding was supported by the Key Research and Development Program of Shaanxi Province (Grant No. 2020ZDLSF04-07), the National Key Research and Development Program of China (Grant No. 2019QY(Y)0502), the National Natural Science Foundation of China (Grant No. 51905438), the Innovation Platform of Biofabrication (Grant No. 17SF0002) and the Fundamental Research Funds for the Central Universities (Grant No. 31020190502009).

Author contributions YW was involved in conception, supervision and modification; YG helped in preparation, analysis and accomplishment; QW and XL contributed to analysis and modification; KJ and KZ were involved in data category and graph editing.

Availability of data and material The datasets generated in this review are available in Web of Science, and Elsevier Science Direct.

Compliance with ethics standards

Conflict of interest The authors declare that there is no conflict of interest.

Consent to participate Not applicable.

Consent for publication Not applicable.

Ethical approval This study does not contain any studies with human or animal subjects performed by any of the authors.

References

1. Filardo G, Vannini F, Marcacci M et al (2013) Matrix-assisted autologous chondrocyte transplantation for cartilage regeneration in osteoarthritic knees: results and failures at midterm follow-up. Am J Sports Med 41(1):95–100. https://doi.org/10.1177/0363546512463675
2. Eldracher M, Orth P, Cucchiarini M et al (2014) Small subchondral drill holes improve marrow stimulation of articular cartilage defects. Am J Sports Med 42(11):2741–2750. https://doi.org/10.1177/0363546514547029
3. Gobbi A, Karnatzikos G, Kumar A (2014) Long-term results after microfracture treatment for full-thickness knee chondral lesions in athletes. Knee Surg Sports Traumatol Arthrosc 22(9):1986–1996. https://doi.org/10.1016/j.arthro.2014.04.072
4. St-Pierre JP, Gan L, Wang J et al (2012) The incorporation of a zone of calcified cartilage improves the interfacial shear strength between in vitro-formed cartilage and the underlying substrate. Acta Biomater 8(4):1603–1615. https://doi.org/10.1016/j.actbio.2011.12.022
5. Glyn-Jones S, Palmer AJR, Agricola R et al (2015) Osteoarthr Lancet 386:376–387. https://doi.org/10.1016/S0140-6736(14)60802-3
6. Parisi C, Salvatore L, Veschini L et al (2020) Biomimetic gradient scaffold of collagen-hydroxyapatite for osteochondral regeneration. J Tissue Eng 11:1–13. https://doi.org/10.1177/2041731419896068
7. Zhang Y, Wang F, Tan H, Chen G, Guo L, Yang L (2012) Analysis of the mineral composition of the human calcified cartilage zone. Int J Med Sci 9(5):353–360. https://doi.org/10.7150/ijms.4276
8. Doulabi AH, Mequanint K, Mohammadi H (2014) Blends and nano composite biomaterials for articular cartilage tissue engineering. Materials (Basel) 7(7):5327–5355. https://doi.org/10.3390/ma7075327
9. Horner CB, Maldonado M, Tai Y et al (2019) Spatially regulated multiphenotypic differentiation of stem cells in 3D via engineered mechanical gradient. ACS Appl Mater Interfaces 11(49):45479–45488. https://doi.org/10.1021/acsami.9b17266
10. Zhang L, Hu J, Athanasiou KA (2009) The role of tissue engineering in articular cartilage repair and regeneration. Crit Rev Biomed Eng 37(1–2):1–57. https://doi.org/10.1615/CritRevBiomedEng.v37.i1-2.10
11. Korpayev S, Toprak Ö, Kaygusuz G et al (2020) Regulation of chondrocyte hypertrophy in an osteochondral interface mimicking gel matrix. Colloids Surf B 193:111111. https://doi.org/10.1016/j.colsurfb.2020.111111
12. Cai H, Yao Y, Xu Y et al (2019) A Col I and BCP ceramic bilayer scaffold implant promotes regeneration in osteochondral defects. RSC Adv 9(7):3740–3748. https://doi.org/10.1039/C8RA09171D
13. Poole AR, Kojima T, Yasuda T, Mwale F, Kobayashi M, Laverty S (2001) Composition and structure of articular cartilage: a template for tissue repair. Clin Orthop Relat Res 391:26–33. https://doi.org/10.1097/00003086-200110001-00004
14. She H, Xiao X, Liu R (2007) Preparation and characterization of polycaprolactone-chitosan composites for tissue engineering applications. J Mater Sci 42(19):8113–8119. https://doi.org/10.1007/s10853-007-1706-7
15. Xiao H, Huang W, Xiong K et al (2019) Osteochondral repair using scaffolds with gradient pore sizes constructed with silk fibroin, chitosan, and nano-hydroxyapatite. Int J Nanomed 14:2011–2027. https://doi.org/10.2147/IJN.S191627
16. Barr AJ, Dube B, Hensor EMA et al (2016) The relationship between three-dimensional knee MRI bone shape and total knee replacement—a case control study: data from the Osteoarthritis Initiative. Rheumatology 55(9):1585–1593. https://doi.org/10.1093/rheumatology/kew191
17. Stocco TD, Antonioli E, Elias CMV et al (2019) Cell viability of porous poly (d, l-lactic acid)/vertically aligned carbon nanotubes/nanohydroxyapatite scaffolds for osteochondral tissue engineering. Materials 12(6):849. https://doi.org/10.3390/ma12060849
18. Yujiao X, Xiaofeng L, Zhuang H et al (2018) Synthesis, self-assembly, and drug-release properties of new amphipathic liquid crystal polycarbonates. Nanomaterials 8(4):195. https://doi.org/10.3390/nano8040195
19. Liu W, Lipner J, Xie J et al (2014) Nanofiber scaffolds with gradients in mineral content for spatial control of osteogenesis. ACS Appl Mater Interfaces 6(4):2842–2849. https://doi.org/10.1021/am405418g
20. Lin X, Chen J, Qiu P et al (2018) Biphasic hierarchical extracellular matrix scaffold for osteochondral defect regeneration. Osteoarthr Cartil 26(3):433–444. https://doi.org/10.1016/j.joca.2017.12.001
21. Oegema TR, Carpenter RJ, Hofmeister F et al (1997) The interaction of the zone of calcified cartilage and subchondral bone in osteoarthritis. Microsc Res Tech 37(4):324–332. https://doi.org/10.1002/(SICI)1097-0029(19970515)37:4%3C324::AID-JEMT7%3E3.0.CO;2-K

22. Langer R, Tirrell DA (2004) Designing materials for biology and medicine. Nature 428(6982):487–492. https://doi.org/10.1038/nature02388
23. Zhang S, Chen L, Jiang Y et al (2013) Bi-layer collagen/microporous electrospun nanofiber scaffold improves the osteochondral regeneration. Acta Biomater 9(7):7236–7247. https://doi.org/10.1016/j.actbio.2013.04.003
24. Rene ON, Lee EM, Kathryn S et al (2017) Substrate stiffness controls osteoblastic and chondrocytic differentiation of mesenchymal stem cells without exogenous stimuli. PLoS ONE 12(1):e0170312. https://doi.org/10.1371/journal.pone.0170312
25. Maheshwari SU et al (2014) Fabrication and evaluation of (PVA/HAp/PCL) bilayer composites as potential scaffolds for bone tissue regeneration application. Ceram Int 40(6):8469–847. https://doi.org/10.1016/j.ceramint.2014.01.0587
26. Schaefer D, Martin I, Jundt G et al (2002) Tissue-engineered composites for the repair of large osteochondral defects. Arthritis Rheumatol 46(9):2524–2534. https://doi.org/10.1002/art.10493
27. Erickson AE, Sun J, Lan Levengood SK et al (2019) Chitosan-based composite bilayer scaffold as an in vitro osteochondral defect regeneration model. Biomed Microdevice 21(2):21–34. https://doi.org/10.1007/s10544-019-0373-1
28. Chaudhuri O, Gu L, Klumpers D et al (2016) Hydrogels with tunable stress relaxation regulate stem cell fate and activity. Nat Mater 15(3):326–334. https://doi.org/10.1038/nmat4489
29. Chen J, Chin A, Almarza A et al (2019) Hydrogel to guide chondrogenesis versus osteogenesis of mesenchymal stem cells for fabrication of cartilaginous tissues. Biomed Mater 15(4):045006. https://doi.org/10.1088/1748-605X/ab401f
30. Lake GJ, Thomas AG (1967) The strength of highly elastic materials. Proceedings A 300(1460):108–119. https://doi.org/10.1098/rspa.1967.0160
31. Dai W, Kawazoe N, Lin X et al (2010) The influence of structural design of PLGA/collagen hybrid scaffolds in cartilage tissue engineering. Biomaterials 31(8):2141–2152. https://doi.org/10.1016/j.biomaterials.2009.11.070
32. Okumura Y, Ito K et al (2001) The polyrotaxane gel: a topological gel by figure-of-eight cross-links. Adv Mater 13(7):485–487. https://doi.org/10.1002/1521-4095(200104)13:7%3C485::aid-adma485%3E3.0.co;2-t
33. Laurenti M, Al Subaie AE, Abdallah MN et al (2016) 2D magnesium phosphate nanosheets form highly thixotropic gels that up-regulate bone formation. Nano Lett 16:4779–4787. https://doi.org/10.1021/acs.nanolett.6b00636
34. Haraguchi K, Takehisa T (2002) Nanocomposite hydrogels: a unique organic-inorganic network structure with extraordinary mechanical, optical, and swelling/deswelling properties. Adv Mater 14(16):1120–1124. https://doi.org/10.1002/1521-4095(20020816)14:16%3C1120::AID-ADMA1120%3E3.0.CO;2-9
35. Santis RD, Gloria A, Russo T et al (2013) Advanced composites for hard-tissue engineering based on PCL/organic–inorganic hybrid fillers: from the design of 2D substrates to 3D rapid prototyped scaffolds. Polym Compos 34(9):1413–1417. https://doi.org/10.1002/pc.22446
36. Stocco TD, Antonioli E, Elias CDV et al (2019) Cell viability of porous poly (d, l-lactic acid)/vertically aligned carbon nanotubes/nanohydroxyapatite scaffolds for osteochondral tissue engineering. Materials 12:1944–1996. https://doi.org/10.3390/ma12060849
37. Liu JY, Li L, Suo HR et al (2019) 3D printing of biomimetic multi-layered GelMA/nHA scaffold for osteochondral defect repair. Mater Des 171:107708. https://doi.org/10.1016/j.matdes.2019.107708
38. Zhang K, He S, Yan S et al (2016) Regeneration of hyaline-like cartilage and subchondral bone simultaneously by poly(L-glutamic acid) based osteochondral scaffolds with induced autologous adipose derived stem cells. J Mater Chem B 15(4):2628–2645. https://doi.org/10.1039/c5tb02113h
39. Zhou X, Esworthy T et al (2019) 3D printed scaffolds with hierarchical biomimetic structure for osteochondral regeneration. Nanomed Nanotechnol Biol Med 19:58–70. https://doi.org/10.1016/j.nano.2019.04.002
40. Zhou M, Lozano N, Wychowaniec JK et al (2019) Graphene oxide: A growth factor delivery carrier to enhance chondrogenic differentiation of human mesenchymal stem cells in 3D hydrogels. Acta Biomater 96:271–280. https://doi.org/10.1016/j.actbio.2019.07.027
41. Korpayev S, Kaygusuz G, Şen M et al (2020) Chitosan/collagen based biomimetic osteochondral tissue constructs: a growth factor-free approach. Int J Biol Macromol 156:681–690. https://doi.org/10.1016/j.ijbiomac.2020.04.109
42. Levingstone TJ, Thompson E, Matsiko A et al (2015) Multi-layered collagen-based scaffolds for osteochondral defect repair in rabbits. Acta Biomater 32:149–160. https://doi.org/10.1016/j.actbio.2015.12.034
43. Zhu Y, Kong L, Farhadi F et al (2018) An injectable continuous stratified structurally and functionally biomimetic construct for enhancing osteochondral regeneration. Biomaterials 192:149–158. https://doi.org/10.1016/j.biomaterials.2018.11.017
44. Dong Y, Sun X, Zhang Z et al (2020) Regional and sustained dual-release of growth factors from biomimetic tri-layered scaffolds for the repair of large-scale osteochondral defects. Appl Mater Today 19:100548. https://doi.org/10.1016/j.apmt.2019.100548
45. Chen T, Bai J, Tian J et al (2018) A single integrated osteochondral in situ composite scaffold with a multi-layered functional structure. Colloids Surf B 167:354–363. https://doi.org/10.1016/j.colsurfb.2018.04.029
46. Nukavarapu SP, Dorcemus DL (2013) Osteochondral tissue engineering: current strategies and challenges. Biotechnol Adv 31(5):706–721. https://doi.org/10.1016/j.biotechadv.2012.11.004
47. Kosik-Kozioł A, Costantini M, Mróz A et al (2019) 3D bioprinted hydrogel model incorporating β-tricalcium phosphate for calcified cartilage tissue engineering. Biofabrication 11(3):035016. https://doi.org/10.1088/1758-5090/ab15cb
48. Lin R, Deng C, Li X et al (2019) Copper-incorporated bioactive glass-ceramics inducing anti-inflammatory phenotype and regeneration of cartilage/bone interface. Theranostics 9(21):6300–6313. https://doi.org/10.7150/thno.36120
49. Ghosal K, Bhattacharjee U, Sarkar K (2020) Facile green synthesis of bioresorbable polyester from soybean oil and recycled plastic waste for osteochondral tissue regeneration. Eur Polym J 122:109338. https://doi.org/10.1016/j.eurpolymj.2019.109338
50. Bailey BM, Nail LN, Grunlan MA (2013) Continuous gradient scaffolds for rapid screening of cell–material interactions and interfacial tissue regeneration. Acta Biomater 9(9):8254–8261. https://doi.org/10.1016/j.actbio.2013.05.012
51. Guo J, Li C, Ling S et al (2017) Multiscale design and synthesis of biomimetic gradient protein/biosilica composites for interfacial tissue engineering. Biomaterials 145:44–55. https://doi.org/10.1016/j.biomaterials.2017.08.025
52. Presley G, Shanna Y, Jeffrey H et al (2017) Spatial regulation of bone morphogenetic proteins (BMPs) in postnatal articular and growth plate cartilage. PLoS ONE 12(5):e0176752. https://doi.org/10.1371/journal.pone.0176752
53. Li C, Armstrong JP, Pence IJ et al (2018) Glycosylated superparamagnetic nanoparticle gradients for osteochondral tissue engineering. Biomaterials 176:24–33. https://doi.org/10.1016/j.biomaterials.2018.05.029
54. Levingstone TJ, Matsiko A, Dickson GR et al (2014) A biomimetic multi-layered collagen-based scaffold for

osteochondral repair. Acta Biomater 10(5):1996–2004. https://doi.org/10.1016/j.actbio.2014.01.005
55. Lantada AD, Iniesta HA (2016) Composite scaffolds for osteochondral repair obtained by combination of additive manufacturing, leaching processes and hMSC-CM functionalization. Mater Sci Eng C Mater Biol Appl 59:218–227. https://doi.org/10.1016/j.msec.2015.10.015
56. Annabi N, Nichol JW, Zhong X et al (2010) Controlling the porosity and microarchitecture of hydrogels for tissue engineering. Tissue Eng Part B 16(4):371–383. https://doi.org/10.1089/ten.TEB.2009.0639
57. Sobral JM, Caridade SG, Sousa RA et al (2011) Three-dimensional plotted scaffolds with controlled pore size gradients: effect of scaffold geometry on mechanical performance and cell seeding efficiency. Acta Biomater 7(3):1009–1018. https://doi.org/10.1016/j.actbio.2010.11.003
58. Duan P, Pan Z, Cao L et al (2019) Restoration of osteochondral defects by implanting bilayered poly(lactide-co-glycolide) porous scaffolds in rabbit joints for 12 and 24 weeks. J Orthop Transl 19:68–80. https://doi.org/10.1016/j.jot.2019.04.006
59. Artel A, Mehdizadeh H, Chiu YC et al (2011) An agent-based model for the investigation of neovascularization within porous scaffolds. Tissue Eng Part A 17(17–18):2133–2141. https://doi.org/10.1089/ten.TEA.2010.0571
60. Van der Stok J, Van der Jagt OP, Amin Yavari S et al (2013) Selective laser melting-produced porous titanium scaffolds regenerate bone in critical size cortical bone defects. J Orthop Res 31(5):792–799. https://doi.org/10.1002/jor.22293
61. Huang L, Huang J, Shao H et al (2019) Silk scaffolds with gradient pore structure and improved cell infiltration performance. Mater Sci Eng C 94:179–189. https://doi.org/10.1016/j.msec.2018.09.034
62. Maciulaitis J, Rekštytė S, Bratchikov M et al (2019) Customization of direct laser lithography-based 3D scaffolds for optimized in vivo outcome. Appl Surf Sci 487:692–702. https://doi.org/10.1016/j.apsusc.2019.05.065
63. Yang S, Leong KF, Du Z et al (2004) The design of scaffolds for use in tissue engineering. Part 1. Traditional factors. Tissue Eng 7(6):679–689. https://doi.org/10.1089/107632701753337645
64. Di Luca A, Lorenzo-Moldero I, Mota C et al (2016) Tuning cell differentiation into a 3d scaffold presenting a pore shape gradient for osteochondral regeneration. Adv Healthc Mater 5(14):1753–1763. https://doi.org/10.1002/adhm.201670074
65. Mahapatra C, Kim JJ, Lee JH et al (2019) Differential chondro- and osteo-stimulation in three-dimensional porous scaffolds with different topological surfaces provides a design strategy for biphasic osteochondral engineering. J Tissue Eng 10:1–13. https://doi.org/10.1177/2041731419826433
66. Sophia Fox AJ, Asheesh B, Rodeo SA (2009) The basic science of articular cartilage: structure, composition, and function. Sports Health 1(6):461–468. https://doi.org/10.1016/j.csm.2004.08.007
67. Nowicki M, Zhu W, Sarkar K et al (2019) 3D printing multiphasic osteochondral tissue constructs with nano to micro features via pcl based bioink. Bioprinting 17:e00066. https://doi.org/10.1016/j.bprint.2019.e00066
68. Gonzalez Diaz EC, Shih YR et al (2018) Mineralized biomaterials mediated repair of bone defects through endogenous cells. Tissue Eng Part A 24(13–14):1148–1156. https://doi.org/10.1089/ten.TEA.2017.0297
69. Heemin K, Yuze Z, Shyni V (2018) Functionally graded multilayer scaffolds for in vivo osteochondral tissue engineering. Acta Biomater 78:365–377. https://doi.org/10.1016/j.actbio.2018.07.039
70. Chan EF, Liu I, Semler EJ et al (2012) Association of 3-dimensional cartilage and bone structure with articular cartilage properties in and adjacent to autologous osteochondral grafts after 6 and 12 months in a goat model. Cartilage 3(3):255–266. https://doi.org/10.1177/1947603511435272
71. Subramony SD, Dargis BR, Castillo M et al (2013) The guidance of stem cell differentiation by substrate alignment and mechanical stimulation. Biomaterials 34(8):1942–1953. https://doi.org/10.1016/j.biomaterials.2012.11.012
72. Shuaijun J, Jing W, Ting Z et al (2018) Multilayered scaffold with a compact interfacial layer enhances osteochondral defect repair. ACS Appl Mater Interfaces 10(24):20296–20305. https://doi.org/10.1021/acsami.8b03445
73. Zhang W, Lian Q, Li D et al (2015) The effect of interface microstructure on interfacial shear strength for osteochondral scaffolds based on biomimetic design and 3D printing. Mater Sci Eng C 46:10–15. https://doi.org/10.1016/j.msec.2014.09.042
74. Nowicki MA, Castro NJ, Plesniak MW et al (2016) 3D printing of novel osteochondral scaffolds with graded microstructure. Nanotechnology 27(41):414001. https://doi.org/10.1088/0957-4484/27/41/414001
75. Zhang B, Guo L, Chen H et al (2020) Finite element evaluations of the mechanical properties of polycaprolactone/hydroxyapatite scaffolds by direct ink writing: effects of pore geometry. J Mech Behav Biomed Mater 104:103665. https://doi.org/10.1016/j.jmbbm.2020.103665
76. Bittner SM, Smith BT, Diaz-Gomez L et al (2019) Fabrication and mechanical characterization of 3D printed vertical uniform and gradient scaffolds for bone and osteochondral tissue engineering. Acta Biomater 90:37–48. https://doi.org/10.1016/j.actbio.2019.03.041
77. Liu F, Mao Z, Zhang P et al (2018) Functionally graded porous scaffolds in multiple patterns: new design method, physical and mechanical properties. Mater Des 160:849–860. https://doi.org/10.1016/j.matdes.2018.09.053
78. Fei L, David Z, Peng Z et al (2018) Mechanical properties of optimized diamond lattice structure for bone scaffolds fabricated via selective laser melting. Materials 11(3):374. https://doi.org/10.3390/ma11030374
79. Lacroix D, Planell JA, Prendergast PJ (2009) Computer-aided design and finite-element modelling of biomaterial scaffolds for bone tissue engineering. Philos Trans Math Phys Eng Sci 367(1895):1993–2000. https://doi.org/10.1098/rsta.2009.0024
80. Cahill S, Lohfeld S, Mchugh PE (2009) Finite element predictions compared to experimental results for the effective modulus of bone tissue engineering scaffolds fabricated by selective laser sintering. J Mater Sci Mater Med 20:1255–1262. https://doi.org/10.1007/s10856-009-3693-5
81. Vahdati A, Zhao Y, Ovaert TC et al (2012) Computational investigation of fibrin mechanical and damage properties at the interface between native cartilage and implant. J Biomech Eng 134(11):111004. https://doi.org/10.1115/1.4007748
82. Kinneberg KRC, Nelson A, Stender ME et al (2015) Reinforcement of mono- and bi-layer poly (ethylene glycol) hydrogels with a fibrous collagen scaffold. Ann Biomed Eng 43(11):2618–2629. https://doi.org/10.1007/s10439-015-1337-0
83. Afshar M, Anaraki AP, Montazerian H (2018) Compressive characteristics of radially graded porosity scaffolds architectured with minimal surfaces. J Books 92:254–267. https://doi.org/10.1016/j.msec.2018.06.051
84. San Cheong V, Fromme P, Mumith A et al (2018) Novel adaptive finite element algorithms to predict bone ingrowth in additive manufactured porous implants. J Mech Behav Biomed Mater 87:230–239. https://doi.org/10.1016/j.jmbbm.2018.07.019
85. Hendrikson WJ, Deegan AJ, Ying Y et al (2017) Influence of additive manufactured scaffold architecture on the distribution of surface strains and fluid flow shear stresses and expected osteochondral cell differentiation. Front Bioeng Biotechnol 5:00006. https://doi.org/10.3389/fbioe.2017.00006

86. Haque MA, Kurokawa T, Gong JP (2012) Super tough double network hydrogels and their application as biomaterials. Polymer 53:1805–1822. https://doi.org/10.1016/j.polymer.2012.03.013
87. Zhang P, Liu J, To AC (2016) Role of anisotropic properties on topology optimization of additive manufactured load bearing structures. Scripta Mater 135:148–152. https://doi.org/10.1016/j.scriptamat.2016.10.021
88. Byrne DP, Lacroix D, Planell J et al (2007) Simulation of tissue differentiation in a scaffold as a function of porosity, Young's modulus and dissolution rate: application of mechanobiological models in tissue engineering. Biomaterials 28:5544–5554. https://doi.org/10.1016/j.biomaterials.2007.09.003
89. Checa S, Prendergast PJ (2010) Effect of cell seeding and mechanical loading on vascularization and tissue formation inside a scaffold: a mechano-biological model using a lattice approach to simulate cell activity. J Biomech 43(5):961–968. https://doi.org/10.1016/j.jbiomech.2009.10.044
90. Sen S, Engler AJ, Discher DE (2009) Matrix strains induced by cells: computing how far cells can feel. Cell Mol Bioeng 2(1):39–48. https://doi.org/10.1007/s12195-009-0052-z
91. Olivares AL, Marsal È, Planell JA et al (2009) Finite element study of scaffold architecture design and culture conditions for tissue engineering. Biomaterials 30(30):6142–6149. https://doi.org/10.1016/j.biomaterials.2009.07.041
92. Sandino C, Lacroix D (2011) A dynamical study of the mechanical stimuli and tissue differentiation within a CaP scaffold based on micro-CT finite element models. Biomech Model Mechanobiol 10(4):565–576. https://doi.org/10.1007/s10237-010-0256-0
93. Kandel RA, Grynpas M, Pilliar R et al (2006) Repair of osteochondral defects with biphasic cartilage-calcium polyphosphate constructs in a Sheep model. Biomaterials 27(22):4120–4131. https://doi.org/10.1016/j.biomaterials.2006.03.005
94. Liverani L, Roether JA, Nooeaid P et al (2012) Simple fabrication technique for multilayered stratified composite scaffolds suitable for interface tissue engineering. Mater Sci Eng A 557:54–58. https://doi.org/10.1016/j.msea.2012.05.104
95. Li Z, Jia S, Xiong Z et al (2018) 3D-printed scaffolds with calcified layer for osteochondral tissue engineering. J Biosci Bioeng 126:389–396. https://doi.org/10.1016/j.jbiosc.2018.03.014
96. Harley BA, Lynn AK, Wissner-Gross Z et al (2010) Design of a multiphase osteochondral scaffold III: fabrication of layered scaffolds with continuous interfaces. J Biomed Mater Res Part A 92(3):1078–1093. https://doi.org/10.1002/jbm.a.32387
97. Phillips JE, Burns KL, Doux JML et al (2008) Engineering graded tissue interfaces. Proc Natl Acad Sci USA 105(34):12170–12175. https://doi.org/10.1073/pnas.0801988105
98. Pratap SY, Christakiran MJ, Bhunia BK et al (2018) Hierarchically structured seamless silk scaffolds for osteochondral interface tissue engineering. J Mater Chem B 6(36):5671–5688. https://doi.org/10.1039/C8TB01344F
99. Olubamiji AD, Izadifar Z, Si JL et al (2016) Modulating mechanical behaviour of 3D-printed cartilage-mimetic PCL scaffolds: influence of molecular weight and pore geometry. Biofabrication 8(2):025020. https://doi.org/10.1088/1758-5090/8/2/025020
100. Nakano T, Ishimoto T (2015) Powder-based additive manufacturing for development of tailor-made implants for orthopedic applications. Powder Part 32:75–84. https://doi.org/10.14356/kona.2015015
101. Du Y, Liu H, Yang Q et al (2017) Selective laser sintering scaffold with hierarchical architecture and gradient composition for osteochondral repair in rabbits. Biomaterials 137:37–48. https://doi.org/10.1016/j.biomaterials.2017.05.021
102. Hu XY, Man Y, Li WF et al (2019) 3D bio-printing of CS/Gel/HA/Gr hybrid osteochondral scaffolds. Polymers 11(10):1601. https://doi.org/10.3390/polym11101601
103. Hong S, Sycks D, Chan HF et al (2015) 3D printing of highly stretchable and tough hydrogels into complex, cellularized structures. Adv Mater 27:4035–4040. https://doi.org/10.1002/adma.201570182
104. Zhai X, Ma Y, Hou C et al (2017) 3D-printed high strength bioactive supramolecular polymer/clay nanocomposite hydrogel scaffold for bone regeneration. ACS Biomater Sci Eng 3(6):1109–1118. https://doi.org/10.1021/acsbiomaterials.7b00224
105. Li Z, Jia S et al (2018) 3D-printed scaffolds with calcified layer for osteochondral tissue engineering. J Biosci Bioeng 126(3):389–396. https://doi.org/10.1016/j.jbiosc.2018.03.014
106. Gao F, Xu Z, Liang Q et al (2018) Direct 3D printing of high strength biohybrid gradient hydrogel scaffolds for efficient repair of osteochondral defect. Adv Funct Mater 28(13):1706644. https://doi.org/10.1002/adfm.201706644
107. Idaszek J, Costantini M, Karlsen TA et al (2019) 3D bioprinting of hydrogel constructs with cell and material gradients for the regeneration of full-thickness chondral defect using a microfluidic printing head. Biofabrication 11(4):044101. https://doi.org/10.1088/1758-5090/ab2622
108. Duarte Campos DF, Blaeser A, Weber M et al (2013) Three-dimensional printing of stem cell-laden hydrogels submerged in a hydrophobic high-density fluid. Biofabrication 5(1):015003. https://doi.org/10.1088/1758-5082/5/1/015003
109. Highley CB, Rodell CB, Burdick JA (2015) Direct 3D printing of shear-thinning hydrogels into self-healing hydrogels. Adv Mater 27(34):5075–5079. https://doi.org/10.1002/adma.201501234
110. Bhattacharjee T, Zehnder SM, Rowe KG et al (2015) Writing in the granular gel medium. Sci Adv 1(8):e1500655. https://doi.org/10.1126/sciadv.1500655
111. Senior JJ, Cooke ME, Grover LM et al (2019) Fabrication of complex hydrogel structures using suspended layer additive manufacturing (SLAM). Adv Mater 29(49):1904845. https://doi.org/10.1002/adfm.201904845
112. Zhou X, Nowicki M, Cui H et al (2017) 3D bioprinted graphene oxide-incorporated matrix for promoting chondrogenic differentiation of human bone marrow mesenchymal stem cells. Carbon 116:615–624. https://doi.org/10.1016/j.carbon.2017.02.049
113. Zhou X, Cui H, Nowicki M, Miao S, Lee SJ, Masood F et al (2018) Three dimensional-bioprinted dopamine-based matrix for promoting neural regeneration. ACS Appl Mater Interfaces 10:8993–9001. https://doi.org/10.1021/acsami.7b18197
114. Wu X, Lian Q, Li D et al (2019) Biphasic osteochondral scaffold fabrication using multi-material mask projection stereolithography. Rapid Prototyp J 25(2):277–288. https://doi.org/10.1108/RPJ-07-2017-0144
115. Gao F, Xu Z, Liang Q et al (2019) Osteochondral regeneration with 3D-printed biodegradable high-strength supramolecular polymer reinforced-gelatin hydrogel scaffolds. Adv Sci 6(15):1900867. https://doi.org/10.1002/advs.201900867
116. Li L, Li J, Guo J et al (2019) 3D molecularly functionalized cell-free biomimetic scaffolds for osteochondral regeneration. Adv Funct Mater 29(6):1807356. https://doi.org/10.1002/adfm.201807356
117. Daly AC, Kelly DJ (2019) Biofabrication of spatially organised tissues by directing the growth of cellular spheroids within 3D printed polymeric microchambers. Biomaterials 197:194–206. https://doi.org/10.1016/j.biomaterials.2018.12.028
118. Di Luca A, Van Blitterswijk C, Moroni L (2015) The osteochondral interface as a gradient tissue: from development to the fabrication of gradient scaffolds for regenerative medicine. Birth Defects Res C Embryo Today Rev 105(1):34–52. https://doi.org/10.1002/bdrc.21092
119. Scotti C, Wirz D, Wolf F et al (2010) Engineering human cell-based, functionally integrated osteochondral grafts by biological bonding of engineered cartilage tissues to bony scaffolds.

Biomaterials 31(8):2252–2259. https://doi.org/10.1016/j.biomaterials.2009.11.110

120. Kuang L, Ma X, Ma Y et al (2019) Self-assembled injectable nanocomposite hydrogels coordinated by in situ generated CaP nanoparticles for bone regeneration. ACS Appl Mater Interfaces 11(19):17234–17246. https://doi.org/10.1021/acsami.9b03173
121. Shao L, Gao Q, Xie C et al (2020) Sacrificial microgel-laden bioink-enabled 3D bioprinting of mesoscale pore networks. Bio Des Manuf 3(1):30–39. https://doi.org/10.1007/s42242-020-00062-y
122. Shao L, Gao Q, Xie CQ et al (2019) Synchronous 3D bioprinting of large-scale cell-laden constructs with nutrient networks. Adv Healthc Mater 9(15):1901142. https://doi.org/10.1002/adhm.201901142